Sl. No.	IIT Ropar List of Recent Publications with Abstract Coverage: April, 2026
A	**Book Chapter(s)**
1.	Digital entomology: Revolutionising biodiversity management in Indian agriculture A Bhardwaj, **MS Badwal, S Sharma, R Trikha, S Kumar, PP Singh** - Harvesting Intelligence: The AI Revolution in Agriculture: From Fields to Algorithms, Cultivating Future Harvests: Book Chapter, 2026 **Abstract:** India's agricultural sector is undergoing a critical transformation to meet the dual challenges of ensuring food security for a growing population and conserving rapidly declining biodiversity. Traditional methods of insect biodiversity monitoring, often manual, labour-intensive, and limited in scale, are proving inadequate in the face of emerging threats such as climate change, pollinator decline, and pest outbreaks. This chapter presents a case study of the *Biodiversity Sensor*, a cutting-edge solution developed by *the Indian Institute of Technology (IIT) Ropar*. The Biodiversity Sensor is a solar-powered, AI-enabled, and field-deployable device capable of autonomously detecting, classifying, and quantifying insect species with over 90% accuracy. Built using *YOLOv5 deep learning architecture*, motion-sensing cameras, and IoT connectivity, the sensor facilitates real-time data collection and cloud-based analytics. Initially focused on monitoring *bee pollinators*, it now supports broader applications in *precision pest management*, *pollinator conservation*, and *biodiversity indexing* across diverse farm ecosystems. The device has been successfully deployed in over 10 countries, including India, the USA, Germany, and Australia, demonstrating its scalability and adaptability to different agricultural contexts. This chapter explores the sensor's technological design, training methodology, deployment strategy, and socio-economic impact. It highlights how digital entomology is revolutionising smart agriculture by turning silent ecosystems into data-rich landscapes. By empowering farmers, researchers, and policymakers with actionable biodiversity insights, the Biodiversity Sensor stands as a scalable model for *data-driven, climate-resilient, and sustainable agriculture*, contributing meaningfully to India's vision for precision farming and ecological stewardship.
2.	Effect of various parameters on shape recovery of shape memory alloys T Talapaneni, V Chaturvedi, RK Sahu, **A Lavakumar** - Sustainability of Alloys and Polymers of Shape Memory Materials: Book Chapter, 2026 **Abstract**: Shape memory alloys (SMAs) are unique materials capable of returning to their predeformed shape upon exposure to specific stimuli, such as temperature changes or applied stress. This intrinsic property is exploited in numerous applications, including medical devices, aerospace components, and automotive systems. Various parameters significantly influence the effectiveness and efficiency of shape recovery in SMAs. This chapter explores the impact of critical parameters like thermal parameters (transformation temperature, thermal cycling), mechanical parameters (stress applied, deformation mode), material composition and processing (alloy composition, heat treatment, microstructure), and environmental factors (ambient conditions, surface treatments) on the shape recovery behavior of SMAs. Understanding the effects of these parameters is vital for optimizing the design and application of SMAs in various industries. By systematically controlling and tailoring these factors, it is possible to enhance the performance, reliability, and longevity of SMAs in their respective applications. Further research into the synergistic effects of these parameters will continue to advance the field, leading to innovative and improved uses of SMAs.

3.	Ionic liquids: Alternative to conventional molecular solvents for organic reactions **A Singh,** S Baskar, C Baskar - Ionic Liquids, Nanofluids and Nanotechnology: Innovations, Applications and Sustainability: Book Chapter, 2026 **Abstract:** Ionic liquids (ILs) are typically characterized as ionic compounds that possess a melting point less than 100 °C. The first IL was ethyl ammonium nitrate which was identified in 1914 by Paul Walden. These substances are recognized for their remarkable performance as chemicals. They exhibit extremely low vapor pressures and can be tailored for specific interactions with various chemicals and materials, including catalysts, solutes, and interfaces involving liquids and gases. ILs demonstrate exceptional thermal and electrochemical stability, and their nucleophilic properties can be finely adjusted. Composed entirely of ions, ILs are increasingly being used as environmentally friendly solvents in numerous organic synthesis processes because their high solvent power and minimal volatility make them a sustainable alternative to traditional volatile molecular solvents in various organic reactions as solvents, catalysts, reagents, or combinations. ILs promote eco-friendliness, sustainability, and principles of the circular economy. Since the ILs line up with the accordance of green chemistry principles, ongoing research into eco-friendly, biodegradable ILs is crucial for their full incorporation into the framework of a circular economy. Their relationship with the circular economy is reinforced through multiple pathways that promote sustainability, improve resource efficiency, and reduce waste. This chapter delivers an inclusive analysis about the necessity and function of ILs in the organic reactions along with a critical discussion on the extent to which ILs can replace conventional solvents.
4.	Nanoformulation triggered by deep eutectic solvents **R Pal, M Prajapati,** Y Vora, K Kuperkar, **D Singh, K Kumar** - Deep Eutectic Solvents: Volume Two: Advanced Applications and Future Perspectives: Book Chapter, 2026 **Abstract:** Nanoformulations, with particle sizes ranging from 10 to 100 nm, were employed to enhance drug delivery by improving solubility, stability, and enabling controlled release. These systems protected therapeutic agents from environmental degradation and facilitated targeted delivery, thereby optimizing therapeutic outcomes with lower dosing requirements. Deep eutectic solvents (DESs) have gained attention as eco-friendly substitutes for traditional solvents in the synthesis of nanomaterials. Owing to their low toxicity, biodegradability, and versatility, DESs enhanced the solubility, stability, and reactivity of nanoparticles, allowing precise control over nanoparticle formation. In this chapter, the use of DESs in synthesizing carbon-based, polymeric, and metal-based nanomaterials was discussed, demonstrating their wide-ranging potential in areas such as biomedicine, catalysis, energy storage, and environmental remediation. The integration of DESs with nanotechnology fostered sustainable innovation, paving the way for cleaner and more efficient advancements in materials science.
5.	Pesticide contamination in soil and water: Type of pesticide, route of expose, and its toxic impacts P Yadav…**A Das**, G Tripathi, Ashish, A Farooqui - Environmental Toxicology and Human Health: Current Challenges and Future Perspectives: Book Chapter, 2026 **Abstract:** One important concept in the sphere of agricultural development is pesticides. Consequently, the use of pesticides results in both acute and chronic toxicities in humans, and their detrimental impacts on the environment along with human health continue to be major concerns in the modern world. Therefore, there needs to be discussion about the methods for applying pesticides, the routes *via* which they are exposed to them, and the health hazards connected to their use. The health dangers posed by pesticide applications and exposure in developing countries are among the primary concerns. In addition to being physically exposed to pesticides through their work in agriculture and the home, along with other industries, people were also exposed indirectly to them through environmental media, for example, food, trash, and soil. The pesticides were

	administered to humans orally, respiratorily, and topically. Humans who are indirectly or directly exposed to pesticides may contract the effects of acute toxicity as well as chronic diseases.
6.	Phase transformation phenomena in shape memory alloys **SP Mohapatra, AK Patro,** V Chaturvedi, T Talapaneni, **A Lavakumar** - Sustainability of Alloys and Polymers of Shape Memory Materials: Book Chapter, 2026 **Abstract:** This chapter delves into the intricate phase transformation phenomena in shape memory alloys (SMAs), materials renowned for their unique ability to return to a predefined shape upon heating. We begin by outlining the fundamental principles of phase transformations, including the martensitic and reverse transformations that underpin the shape memory effect and superelasticity. The chapter explores the thermodynamics and kinetics of these transformations, emphasizing the role of thermal and mechanical stimuli. Detailed discussions on the microstructural changes during phase transformations provide insight into the mechanisms driving the functional properties of SMAs. Furthermore, we examine various alloy systems, highlighting their composition, phase stability, and transformation temperatures. The influence of factors such as alloying elements, thermal treatments, and external stresses on phase transformation behavior is thoroughly analyzed. By integrating experimental findings with theoretical models, this chapter offers a comprehensive understanding of phase transformation phenomena in SMAs, paving the way for advanced applications ranging from biomedical devices to aerospace engineering.
7.	Properties of shape memory alloys V Chaturvedi, RK Sahu, **A Lavakumar,** T Talapaneni - Sustainability of Alloys and Polymers of Shape Memory Materials: Book Chapter, 2026 **Abstract:** Shape memory alloys (SMAs) exhibit unique properties, making them highly valuable in various industrial and medical applications. These materials are characterized by their ability to return to a predeformed shape upon exposure to specific thermal or mechanical stimuli. The critical properties of SMAs include the shape memory effect, pseudoelasticity, and high damping capacity. The shape memory effect is the ability of SMAs to undergo deformation at one temperature and recover their original shape upon heating. This effect is divided into one-way and two-way memory effects, allowing the material to remember and switch between two distinct shapes at different temperatures. Pseudoelasticity, or superelasticity, enables SMAs to resist substantial strains and revert to their original form upon unloading at a constant temperature. Additionally, SMAs exhibit high damping capacity, which makes them effective in absorbing and dissipating energy, thereby reducing vibrations and noise. These properties result from the reversible martensitic transformation within the material's crystal structure. Common SMAs include Ni–Ti (Nitinol), Cu-based, and Fe-based alloys, each offering distinct advantages in terms of mechanical properties, corrosion resistance, and cost-effectiveness. The exceptional properties of SMAs have led to their widespread use in applications such as medical devices, actuators, aerospace components, and vibration dampers. This chapter highlights the fundamental properties of SMAs that underpin their diverse and critical applications in modern technology.
8.	Significance of AI in solar energy conservation and climate change management Akash, S Kumar, R Rajak, **A Kumar,** V Srivastava, D Sahni, R Saxena - Solar Energy Optimization Using Generative Artificial Intelligence: Book Chapter, 2026 **Abstract:** The integration of artificial intelligence (AI) into the solar energy industry is revolutionizing the way we harness and manage this renewable resource. AI-powered solutions are optimizing solar energy production, enhancing reliability, and improving grid integration, all while contributing to climate change mitigation efforts. By analyzing real-time data from various sources, AI can predict weather patterns and adjust solar panel positioning to maximize energy output. Machine learning algorithms can also identify underperforming solar cells and redistribute

	the load, leading to significant improvements in overall energy production. AI is also transforming solar energy maintenance through predictive analytics. By detecting subtle changes in performance, AI can identify potential issues before they escalate, enabling proactive maintenance and extending the lifespan of solar infrastructure. This not only saves costs but also ensures consistent energy production, contributing to the reliability and sustainability of solar power. Moreover, AI is playing a crucial role in enhancing grid integration and energy storage. By predicting and coordinating solar energy production with other energy sources, AI can ensure a stable power supply and manage the variability inherent in solar power generation. In energy storage, AI is optimizing the use of batteries to store excess solar energy, improving the overall efficiency of solar energy systems and enhancing grid stability. The impact of AI in solar energy extends beyond optimization and maintenance. AI-powered models are being used to map utility-scale solar projects, revealing potential land use conflicts and enabling policymakers to make informed decisions. By identifying suitable locations for solar development, such as decommissioned coal mines or degraded lands, AI can help minimize the ecological and agricultural impact of solar projects. In conclusion, the synergy between AI and solar energy represents a significant step forward in our journey towards a sustainable and energy-efficient future. By optimizing production, enhancing reliability, improving grid integration, and enabling strategic siting, AI is revolutionizing the solar energy industry and contributing to the fight against climate change.
9.	Toxicity of heavy metals P Yadav…**A Das**, G Tripathi, Ashish, A Farooqui - Environmental Toxicology and Human Health: Current Challenges and Future Perspectives: Book Chapter, 2026 **Abstract:** Because of their tendency to persist in the atmosphere, their toxicity, and their capacity to bioaccumulate within our bodies, heavy metals are recognized as environmental contaminants. The pollution of the aquatic and terrestrial ecosystems contaminated with hazardous heavy metals is a major environmental concern, with consequences for public health. Heavy metals are generally found in nature, but some of them are derived from so-called anthropogenic sources. The characterization of heavy metals is based on their toxicity to living organisms and their high atomic mass. Most heavy metals can cause atmospheric and environmental pollution and may also be lethal to humans. The combination of heavy metals with various environmental factors, such as soil, air, and water, as well as human beings, can make them more poisonous. Additionally, other living organisms could come into contact with heavy metals *via* the food chain.
B	**Conference Proceeding(s)**
10.	A comparative analysis of near-field wireless power transfer planar coil geometries and optimization for drone charging systems **S Ahamed,** A Kumar**, S Jain, A Sharma** - IEEE Microwaves, Antennas, and Propagation Conference (MAPCON), 2026 **Abstract:** This paper presents a comprehensive analysis and optimization of various planar coil geometries for near-field wireless power transfer (WPT) systems, primarily aimed at enhancing the operational autonomy and charging efficiency of Unmanned Aerial Vehicles (UAVs). Through a rigorous methodology that integrates EM simulations with experimental validation, the magnetic coupling and electrical parameters of configurations such as Square-Square, Square-Circular, Circular-Circular, and Square-Hexagonal pairings were thoroughly investigated. This study reveals the superior performance of Circular-Circular and Square-Hexagonal geometries in achieving higher magnetic coupling, with the number of turns and geometries playing a crucial role in overall system efficiency. The strong corroboration between the simulated results and the empirical measurements confirms the high fidelity of the simulation model, establishing it as a

	robust tool for the design and optimization of WPT coil structures. This research contributes significant insights and a validated framework for developing efficient drone charging solutions.
11.	A novel image-based watermarking method for detecting false data injection in line current differential relays **S Agarwal, K Tony, M Pandit, R Sodhi** - 11th International Conference on Power Systems (ICPS), 2026 **Abstract:** Line current differential relays (LCDRs) are widely used to protect critical transmission lines from internal faults in power systems via local and remote end measurements. Since LCDRs rely on digital communication channels, which, in turn, are vulnerable to cyberattacks, and thus, can be maloperated, leading to a cascaded failure. This paper proposes a novel image-based dynamic watermarking technique to distinguish between actual faults and false data injection attacks (FDIAs) in LCDR. It dynamically embeds the watermark into the remote-end as well as the local-end current measurement signal. After the extraction of the watermarks from the local and remote end signals, the extracted signals are compared to the original embedded watermark using the Damerau-Levenshtein (DL) distance. The final relay logic is developed based on the DL distance. The working of the proposed scheme is tested on PSCAD using the IEEE 14-bus system model.
12.	A sub-1 V analog memristor utilizing rare-earth erbium oxide (Er_2O_3) for energy-efficient in-memory computing M Malhotra, **MS Yadav, B Rawat,** V Balakrishnan - IEEE 7th International Conference on Emerging Electronics (ICEE), 2026 **Abstract:** This work experimentally investigates Er2O3-based memristor as a potential candidate for energy-efficient nonvolatile memory and neuromorphic computing. The results show that Er2O3-based memristor operates at sub-1 V, exhibits reliable bipolar switching driven by oxygen vacancy migration with the endurance over 16,000 cycles. Pulse measurements reveal gradual and analog conductance modulation under low-voltage stimulation, which enables the effective emulation of long-term potentiation and long-term depression. Furthermore, electrode-dependent studies using Au, Pt, Ag, and Al highlight the critical influence of interfacial chemistry and filament dynamics on switching behavior. These results establish Er2O3-based memristor as stable and CMOS-compatible artificial synapses, which provide a pathway toward scalable and energy-efficient neuromorphic hardware.
13.	AgriFed: A federated learning approach for scalable and secure crop disease detection **H Panchariya, N Narwal, F Qadri, R Chakraborty, P Goyal** - Agriculture-Centric Computation (ICA), 2026 **Abstract:** Agriculture plays an important role in global food security, yet crop disease significantly impacts yield and economic stability. Traditional centralized machine learning approaches for crop disease classification, though effective, pose challenges like data privacy, security, and high communication cost. To overcome these issues, this research introduces AgriFed, a federated learning based framework that enables decentralized training while ensuring confidentiality of data and reduction in data sharing cost. We analyze the performance of number of Convolutional Neural Network based architectures, such as VGG16, GoggleNet, DenseNet, ResNet, MobileNet, and EfficientNet for crop disease classification using TOM2024 dataset, which includes images of tomato, onion and maize crops. The results highlight that federated learning not only preserves data privacy but also achieves comparable or better results than centralized learning. Furthermore, this research explores the balance between model complexity and performance, demonstrating that federated learning is a scalable and efficient method for real-

	time disease crop detection. These findings illustrate the potential of federated learning in modernizing the agriculture technology while ensuring the privacy of data.
14.	An oval shaped receiver coil array harvester for efficient wireless charging of drone **S Jain, A Sharma** - IEEE Microwaves, Antennas, and Propagation Conference (MAPCON), 2026 **Abstract**: This paper presents a novel oval-shaped receiver (Rx) coil architecture integrated with rectifier circuits for efficient wireless charging of drones. Unlike conventional planar or circular Rx designs, the proposed oval coils are strategically fixed to the drone legs, maximizing spatial utilization without compromising aerodynamics. A comparative electromagnetic simulation study of single-turn rectangular and circular versus oval-shaped coils reveals a superior quality factor for the latter. To optimize power transfer, the number of turns in each coil is systematically tuned to achieve the desired DC output voltage across the rectifiers. A DC voltage combining strategy is employed to coherently add the outputs of individual coils, significantly enhancing the overall rectified voltage. Experimental validation confirms the system's effectiveness, achieving a high rectified voltage of 22.77 V at a transmitter current of 973.9 mA. The compact, oval-shaped mounted coil configuration enables seamless integration into drone platforms, making it a promising solution for practical mid-range wireless charging applications.
15.	Analyzing communication performance from testbeds to HPC systems: A lab course **H Kaur, S Shashi, U Konduru, S Kumar, B Sodhi, J Singh,** BS Sanjeev - IEEE 32nd International Conference on High Performance Computing, Data and Analytics Workshop (HiPCW), 2026 **Abstract**: High-Performance Computing (HPC) education is often limited by restricted access to large-scale systems, making it challenging for students to gain practical experience. To address this, we have developed a Low-cost Pi-based Instructional Testbed for Experimentation (LITE-Pi), that provides a hands-on environment for exploring HPC concepts such as parallel programming, communication performance, and scalability. Given that scalable performance depends not only on hardware but also on a deep understanding of parallel system behavior, it is essential to train students in practical aspects of HPC through accessible, small-scale platforms. Our experiments show that communication trends on LITE-Pi closely mirror those of a production HPC cluster, although optimal performance parameters differ, highlighting the need for scale-aware optimization. To extend this understanding, we integrate tools such as Netgauge, LLAMP, and LogGOPSim, enabling students to analyze and optimize performance at larger scales. Based on these insights, we propose a 14-week laboratory course focused on practical experimentation and optimization across system scales, helping students develop the analytical and technical skills required for real-world HPC environments. Upon successful completion of the course, students will acquire the expertise required to transfer the skills and insights gained from LITE-Pi to the production-scale system.
16.	Assessment of heavy metal pollution in Delhi's Yamuna River by utilizing the heavy metal pollution index and geospatial methods A Gani, **S Pathak,** A Hussain - IEEE International Geoscience and Remote Sensing Symposium (IGARSS), 2025 **Abstract:** Yamuna is one of North India's major rivers wit significant mythical and sociocultural relevance. Th Heavy Metal Pollution Index (HPI) and geospatial analysi for mapping the spatial distribution of HPI are used in thi study to evaluate the degree of heavy metal pollution in th Yamuna River. In order to find out the concentrations o significant heavy metals (HM), water samples were take from four locations along the Yamuna River. An overal assessment of pollution severity, the HPI was computed and the findings of the study showed that contaminatio levels were significantly higher than allowed limits i several places. The ITO bridge has the highest averag

	concentration of arsenic (As) of 4.0689 mg/L, whereas th Okhla Barrage (OB) has the lowest average concentratio of 0.1739 mg/L. The Wazirabad Barrage (WB) samplin location has the greatest HPI value of 1798.06, while th Nizamuddin Bridge (NB) sampling location has the lowes HPI value of 38.24. The HPI values of all the samplin locations of the study area are in decreasing order of WB ITO Bridge, OB and NB. GIS mapping was used to show spatial trends and identify areas that have significan pollution. When geospatial data and HPI results wer combined, important zones of HM buildup were identified mostly downstream of urban centres and industrial clusters The high concentration of arsenic, lead and mercury amon all the HM was assessed in samples of river Yamuna thu indicating the river water to be disastrous. The presen study emphasizes that to protect public health and restor the biological balance of the Yamuna River, immediat mitigation measures, stronger pollution control regulations and ongoing monitoring are required.
17.	Benchmarking machine learning algorithms for intrusion detection in UAV communication networks **H Yadav,** S Goswami, **JM Mudiraj, P Rawat, G Yadav,** S Pal - International Conference on Advanced Networks and Telecommunications Systems (ANTS), 2026 **Abstract:** This work investigates the current security landscape of Unmanned Aerial Vehicle (UAV) communication networks by analyzing multiple publicly available UAV-related intrusion detection datasets. Our primary focus is on the recently released UAV-NIDD dataset, which is designed to support intrusion detection system (IDS) development for UAV networks by capturing a wide range of attack scenarios. Prior studies train separate models for individual attack types. Our novelty is that we propose a unified multiclass classification approach to detect all attack categories simultaneously. This presents a more realistic and challenging problem, offering deeper insights into the dataset's capability to represent complex and overlapping attack patterns. We implemented and evaluated numerous machine learning algorithms, including Logistic Regression, Decision Tree, Random Forest, and XGBoost, to assess their effectiveness. The UAV-NIDD dataset includes diverse cyberattack types such as Scanning, Reconnaissance, Denial of Service (DoS), Distributed Denial of Service (DDoS), GPS Jamming, Spoofing, Man-in-the-Middle (MITM), Replay, Evil Twin, Brute Force, and Fake Landing Packet attacks. Our study provides a comprehensive benchmark for UAV IDS development and highlights key challenges in multiclass attack detection within UAV communication systems. To enhance model interpretability, we apply Explainable AI (XAI) techniques using SHAP to identify feature contributions across attack classes. Our analysis reveals key global and local feature influences, particularly for Class 2, providing insights to strengthen UAV IDS robustness.
18.	Bluetooth low energy advertising-based polling technique for collision avoidance in WSNs **S Gautam, S Kumar**, EE Tsiropoulou-IEEE Global Communications Conference (GLOBECOM), 2026 **Abstract:** In Wireless Sensor Networks (WSNs) involving frequent transmission of large sensor data, packet collisions degrade the performance and add to the energy consumption of the sensor nodes since they require additional packet retransmissions to compensate data loss. In this paper, applications like livestock health monitoring systems have been targeted that involve frequent transmission of large sized motion data sampled along multiple axes. We choose low power non-connectable Bluetooth Low Energy (BLE) extended advertisements for quick transmission of large sensor data, and propose a non-connectable BLE advertising based polling algorithm for eliminating packet collision. Contrary to the existing polling-based schemes that are implemented at the link layer, this is the first work to propose a broadcast-based polling algorithm for the "application" layer. This facilitates its adaptability with commercially available BLE chips in practical deployments, since it runs on top of the standardized BLE link layer that does not

	implement carrier sensing. It has been shown through real-world experimentation carried out using nRF52832 and nRF52840 SoCs for 5 days, that the proposed polling technique is more effective in networks with higher transmission rates. In a network of 25 nodes transmitting 3,600 bytes every 30 s, with two packet re-transmissions, polling achieves a consistent data delivery success rate between 98-99%, as opposed to nearly 95% achieved without polling in higher (three) re-transmissions. Higher packet delivery rates are achievable in fewer re-transmissions with polling, thus saving power of the sensor nodes.
19.	Deep learning-based spectrum sensing for dynamic spectrum access **S Srivastava, S Arora, S Kalsotra, S Agarwal** - IEEE DELCON-International Conference on Recent Smart Technologies in Engineering for Sustainable Development, 2026 **Abstract:** Efficient spectrum sensing is crucial for cognitive radios to manage available frequency bands effectively. In this study, we propose a new method for spectrum sensing using deep learning, specifically convolutional neural networks (CNNs). Our model is trained on a diverse dataset encompassing various signal types and noise conditions, enabling it to adapt to new, unseen signals. We also explore transfer learning techniques, such as using pre-trained models, to further enhance detection accuracy. Experimental results demonstrate that our approach outperforms traditional methods, achieving superior accuracy in detecting real-world signals. By automating feature extraction and learning from data, our model simplifies the process and reduces the need for specialized knowledge. Overall, our research contributes to advancing spectrum sensing methods, making them more efficient and accessible for cognitive radio applications.
20.	Design and Implementation of an autonomous wireless charging system for low-power drones VK Srivastava, SR Jain, **A Sharma** - IEEE Microwaves, Antennas, and Propagation Conference (MAPCON), 2026 **Abstract**: This paper presents a design strategy of wireless charging systems adequate with self-aligning capabilities for drones suited for applications such as parcel delivery, military surveillance, and smart agriculture. Key components of the wireless power transfer (WPT) system, including a highfrequency inverter, WPT coil setup, and receiver circuitry, are specifically designed for low-power drones. To enable autonomous charging, a steepest gradient algorithm is implemented for a micro-controller within the receiver circuitry, allowing it to intelligently determine its position from receiver voltage samples and align with the transmitter. The system's performance is first evaluated through a circuit simulator, followed by the high-frequency inverter and receiver circuitry fabrication on a low-cost PCB. The coil setup is made with Litz wire, and the performance of the the complete WPT setup is evaluated. Experimental results demonstrate the system's ability to effectively and autonomously charge a cell, drone battery, underscoring the practical potential of the proposed WPT solution.
21.	Design of coplanar waveguide architecture for magnetic tunnel junction arrays in wireless RF sensing applications **AS Sandhu, R Sharma, R Sharma** - IEEE 7th International Conference on Emerging Electronics (ICEE), 2026 **Abstract:** This paper presents a coplanar waveguide (CPW) architecture design for spintronics-based magnetic tunnel junction (MTJ) arrays targeted at Wireless RF Sensing and Energy Harvesting applications. The proposed design addresses critical challenges in impedance matching, electromagnetic coupling, and scalability for MTJ-based RF sensors operating in the GHz frequency range. Through electromagnetic simulation using ANSYS HFSS, we demonstrate improved coupling efficiency between CPW transmission lines and MTJ devices, which provides the potential to achieve enhanced RF-to-DC conversion performance. The optimized architecture features carefully designed CPW dimensions with 50 Ω characteristic impedance (Z_0) while

	minimizing losses. Our approach provides a foundation for scalable to large MTJs for wireless energy harvesting systems capable of converting ambient RF energy into useful DC power through spin-dependent tunneling magneto-resistance effects.
22.	Dual-polarized hexa port simultaneous wireless information and power transfer antenna **SK Gupta,** S Kumar, **A Sharma** - IEEE Microwaves, Antennas, and Propagation Conference (MAPCON), 2026 **Abstract**: The sustainability of Wireless Sensor Networks (WSNs) is often constrained by the limited battery life of IoT sensor nodes and reduced communication efficiency, leading to increased maintenance efforts. To address both power and data transfer requirements simultaneously, a novel hexa-port dual-polarized antenna system is proposed for Simultaneous Wireless Information and Power Transfer (SWIPT). The design integrates four ports configured as a rectenna for Wireless Power Transfer (WPT), while the remaining two ports support Wireless Information Transfer (WIT). The rectenna exhibits a peak gain of 7.5 dBi with a DC beamwidth of 137.2° in the YZ-plane. Additionally, it achieves a power conversion efficiency (PCE) of 59.2 % at a load resistance of 2300Ω, corresponding to a harvested DC power of under a −10 dBm input power. The dualpolarized WIT configuration offers a 100 MHz bandwidth centered at 2.45 GHz, maintaining an input reflection coefficient below −10 dB. Furthermore, mutual coupling between orthogonal WIT ports is effectively suppressed to below −30 dB, enhancing isolation and communication reliability.
23.	Energy consumption analysis for a robotic arm in vertical farming process: an experimental validation **P Verma, E Singla** - International Conference on Agriculture-Centric Computation, 2026 **Abstract:** In this paper, we present torque analysis and energy consumption of a robot assisting in vertical farming processes: seedling, transplanting and harvesting. The task environment was modelled using the MATLAB Toolbox and inverse dynamics calculations were carried out to determine joint torques and power requirements. Numerical simulations were conducted for each task, followed by hardware validation using the conventional four degree of freedom (DoF) Kinova MICO robot to ensure the accuracy of simulated results. To evaluate the system accuracy, the percentage error between the simulation and hardware results was also calculated. This analysis is crucial for optimizing robotic operations, improving energy efficiency and designing sustainable agricultural automation solutions.
24.	FLandroid: Towards federated learning for android edge devices **A Sharma…N Auluck,** Y Simmhan - IEEE 32nd International Conference on High Performance Computing, Data and Analytics Workshop (HiPCW), 2026 **Abstract:** Federated Learning (FL) on mobile devices enables collaborative model training while preserving data privacy, but bringing FL to resource-constrained Android environments requires lightweight solutions. We present Flandroid, a framework that integrates MQTT for efficient server–client communication with TensorFlow Lite for on-device model personalization. Preliminary experiments with models such as MobileNetV2 and DenseNet demonstrate the feasibility of Android clients actively participating in FL rounds, opening avenues for scalable, mobile-first FL deployments.
25.	FreqRec: A lightweight and adaptive LFU-LRU hybrid policy for cache block replacement **T Randive,** K Arvind, DP Bhishmacharya, A Joshi, OB Shinge - IEEE 17th International Conference on Computational Intelligence and Communication Networks (CICN), 2026 **Abstract:** Effective cache replacement policies are necessary to maximise memory subsystem performance in modern processors, especially when workloads exhibit dynamic and varied

	memory access patterns. In mixed-access workloads, traditional methods such as Least Recently Used (LRU) and Least Frequently Used (LFU) are limited by their one-dimensional focus on recency or frequency, which often results in less-than-ideal selections. This study proposes FreqRec, a lightweight hybrid replacement policy that uses both frequency and recency data to maximise cache efficiency with minimal overhead. Performance is evaluated using benchmarks from the SPEC CPU 2017 suite. Experimental results show that FreqRec significantly exceeds LRU, increasing the xalancbmks-202B's instructions per cycle (IPC) by 54.16 percent and MSHR merges in 654.romss-293B is decreased by 2.61 percent, suggesting improved bandwidth utilisation and proving how effectively FreqRec reduces pressure on the memory subsystem. The suggested policy delivers substantial IPC improvements for selected workloads, such as xalancbmks-202B and romss-293 B, showing its strength in exploiting temporal locality. However, streaming-intensive applications like omnetpp and fotonik3d see slight regressions around 4 percent to 6 percent, suggesting opportunities for tuning the policy to better handle such access patterns. These findings demonstrate that FreqRec is a flexible and scalable cache replacement solution that can be incorporated into contemporary multicore architectures for applications requiring high throughput and data volume.
26.	From RF to acoustic: A DL based receiving prototype for underwater acoustic communication **S Kumar, A Ahmad, S Agarwal, S Darshi** - National Conference on Communications (NCC), 2026 **Abstract:** Data decoding in underwater acoustic (UWA) communication is highly challenging due to Doppler shifts and multipath propagation of acoustic signal. With the growing demand for reliable data transmission in UWA systems, accurate data decoding has become essential. Moreover, real time UWA communication systems must be adaptable and optimized according to varying environmental conditions. However, existing techniques remain insufficient to achieve the desired throughput and bit error rate (BER). To address these limitations, this work presents the design, implementation, and experimental evaluation of a deep learning (DL) based algorithm for data decoding, aimed at improving BER and throughput performance. Simulated results with 2dB gain has been demonstrated over existing DL algorithm. Furthermore, the proposed DL algorithm is validated on a hardware setup to assess its practical effectiveness.
27.	High tunneling electroresistance ratio in asymmetric resonant ferroelectric tunnel junctions: Role of quantum well and electrostatics **B Khattar, A Tripathi,** A Sharma - IEEE 7th International Conference on Emerging Electronics (ICEE), 2026 **Abstract:** We investigate electrostatic and material engineering strategies to optimize asymmetric resonant HfO_2-based ferro-electric tunnel junctions for low resistance-area product and high tunneling electroresistance ratios. Using a barrier-well-barrier architecture, we systematically analyze the impact of quantum well (QW) thickness, position, electric permitivity and screening length of electrodes on resonant tunneling performance. Our findings reveal that introducing an asymmetric QW enhances field modulation, while high-permittivity materials such as TiO_2 stabilize polarization and refine band alignment. These combined effects facilitate efficient resonant tunneling, highlighting the potential of multilayer ferroelectric tunnel junctions for scalable non-volatile memory and neuromorphic computing applications.
28.	Improving glacial lake segmentation with slope-awareness and prompt-based sam refinement V Singh, AP Mahadevan, NC Krishnan, **RK Tiwari** - IEEE International Geoscience and Remote Sensing Symposium (IGARSS), 2025 **Abstract:** Accurate glacial lake mapping is crucial for assessing climate change impacts and mitigating Glacial Lake Outburst Flood risks. This study presents a novel framework combining

	the Slope-aware NAU-Net model and the Segment Anything Model (SAM) to address key challenges in glacial lake segmentation. The Slope-aware NAU-Net leverages slope data and NDWI to enhance feature learning, while SAM refines segmentation outputs, resolving incomplete lake boundaries, and improving small lake segmentation. The framework achieves significant performance gains, including an 11.5% IoU improvement for small lakes and 5.6% for larger lakes, setting a new standard for precise and reliable glacial lake mapping.
29.	Investigating the viability of employing multi-modal large language models in the context of audio deepfake detection **A Chuchra,** S Reddy, **S Mishra,** A Das, A Dhall - IEEE International Joint Conference on Biometrics (IJCB), 2026 **Abstract:** While Vision-Language Models (VLMs) and Multimodal Large Language Models (MLLMs) have shown strong generalisation in detecting image and video deepfakes, their use for audio deepfake detection remains largely unexplored. In this work, we aim to explore the potential of MLLMs for audio deepfake detection. Combining audio inputs with a range of text prompts as queries to find out the viability of MLLMs to learn robust representations across modalities for audio deepfake detection. Therefore, we attempt to explore text-aware and context-rich, question-answer based prompts with binary decisions. We hypothesise that such a feature-guided reasoning will help in facilitating deeper multimodal understanding and enable robust feature learning for audio deepfake detection. We evaluate the performance of two MLLMs, Qwen2-Audio-7B-Instruct and SALMONN, in two evaluation modes: (a) zero-shot and (b) fine-tuned. Our experiments demonstrate that combining audio with a multi-prompt approach could be a viable way forward for audio deepfake detection. Our experiments show that the models perform poorly without task-specific training and struggle to generalise to out-of-domain data. However, they achieve good performance on in-domain data with minimal supervision, indicating promising potential for audio deepfake detection.
30.	LoraNet: Robust LoRa signal classification using deep convolutional neural networks and spectrograms **S Srivastava, S Arora, S Kalsotra, S Agarwal** - IEEE International Conference on Recent Smart Technologies in Engineering for Sustainable Development (DELCON), 2026 **Abstract:** LoRa (Long Range) technology is the cornerstone for many Low-Power Wide-Area Network (LPWAN) applications, demanding reliable signal detection for efficient spectrum utilization and robust communication. This paper introduces LoraNet, a Convolutional Neural Network (CNN) specifically designed for the binary classification of LoRa signals—distinguishing LoRa transmissions from Non-LoRa signals (e.g., noise or other interference) using their spectrogram representations. A comprehensive dataset was curated, featuring LoRa signals generated with diverse parameters including spreading factor and bandwidth. These signals, along with Non-LoRa samples consisting of single-tone sine waves, were embedded in additive white Gaussian noise across a challenging signal-to-noise ratio (SNR) range of -30 dB to +10 dB. LoraNet leverages a deep CNN architecture to learn discriminative features from these spectrograms. Experimental results demonstrate strong performance, with LoraNet achieving an overall accuracy of 89.88% on the test set. Notably, it achieves 51.20% accuracy at -30dB SNR, 98.20% at -20dB SNR, and 100.00% accuracy at SNRs of -10 dB and above. This highlights its robustness and effectiveness, particularly in low SNR conditions where traditional signal processing techniques often struggle. This study highlights the efficacy of deep learning in reliably detecting LoRa signal presence within complex radio environments.
31.	Multimodal fusion for cow behavior prediction **A Kumar, A Upadhyay, V Kukreti, V Yashaswini, S Bansal, N Goel, M Saini** - International Conference on Agriculture-Centric Computation, 2026

	Abstract: Conventional livestock monitoring systems often lack the detail and flexibility needed to capture complex animal behavior patterns. In this work, we propose a multimodal learning approach that fuses data from multiple sensor sources for accurate behavior recognition in dairy cows. We use the MMCows dataset, which provides synchronized recordings from diverse modalities. Our method applies supervised learning to individual sensor streams and employs data fusion techniques to combine complementary information for improved behavior classification. We evaluate our multimodal model to measure its generalizability and robustness, achieving the highest F1 scores across all behavior categories. Our work demonstrates the effectiveness of multimodal data fusion in advancing livestock behavior monitoring and supports the development of automated, real-time management systems.
32.	Performance potential of MoS_2-based negative capacitance CFET for the future technology node S Poria, **B Rawat,** G Trivedi - IEEE 7th International Conference on Emerging Electronics (ICEE), 2026 **Abstract:** As CMOS technology scales toward the 1-nm node, Si-based nanosheet FET (NS-FET) architecture, including complementary FET (CFET) inverter, encounters fundamental limitations in drive current and power efficiency. To address these challenges, we present a three-channel stacked MoS_2-based negative capacitance (NC) CFET for the 1-nm technology node using a fully calibrated 3-D TCAD framework. The results show that MoS_2 NC-CFET delivers around 20% higher on-current (I_{on}), about 8% steeper subthreshold swing (SS), and nearly 2× intrinsic DC gain at V_{DS} = 0.7 V, compared to the conventional CFET counterpart. Furthermore, power–frequency analysis of the 17-stage ring oscillator (RO) demonstrates around 14% better energy efficiency under iso-frequency condition. Our research underscores that MoS_2 with stacked NC-CFET offers a promising solution for improving energy efficiency and switching speed at the 1-nm technology node.
33.	PF-MSAS: Multi-split address scheme based LSTM prefetcher with DoA filtering **S Jaiswal, VK Tavva** - IEEE 32nd International Conference on High Performance Computing, Data and Analytics Workshop (HiPCW), 2026 **Abstract:** Graph applications demand low-latency queries and high-throughput analytics but remain memory-bound due to large, irregular access patterns. Although ML-prefetchers like Voyager and TransFetch improve performance, they suffer from high Dead-on-Arrival (DoA) rates and Last Level Cache (LLC) pressure. This work proposes a novel technique, i.e., PF-MSAS, that enhances ML-prefetching by combining address splitting with DoA-aware filtering. An LSTM-based multi-split address model (MSB + LSB + offset) reduces vocabulary size and aliasing, while LLC-level DoA tracking filters ineffective prefetches. The approach improves cache utilization, prefetch accuracy, and overall performance-achieving 48.98% IPC gain over the baseline, 7.48% over Voyager, and 2.44% over TransFetch—demonstrating its potential for efficient cache-aware ML-prefetching.
34.	PPO based real-time beamforming and power splitting in near-field SWIPT systems U Singh…**A Sharma,** V Bhatia - IEEE International Conference on Advanced Networks and Telecommunications Systems (ANTS), 2026 **Abstract:** Near-field wireless communication in millimeter-wave and terahertz systems unlocks high-capacity and energy-efficient connectivity but also introduces new challenges in beamforming and power control due to spherical wavefronts and spatial non-stationarity. This paper presents a near-field constraint-aware proximal policy optimization (NF-CA-PPO) framework for simultaneous wireless information and power transfer (SWIPT) in a multi-transmitter environment. The proposed learning framework formulates joint beamforming and

	power-splitting optimization as a Markov Decision Process (MDP) and integrates constraint satisfaction directly into the policy learning stage through projection-based and penalty-aware updates. Unlike conventional convex optimization or standard deep reinforcement learning (DRL) methods, NF-CA-PPO guarantees physical feasibility, improves sample efficiency, and achieves real-time adaptability under near-field channel variations. Simulation results show that NF-CA-PPO reduces total transmit power and attains faster, more stable convergence than baseline (deep deterministic policy gradient), while consistently satisfying signal-to-interference-plus-noise ratio (SINR) and energy-harvesting constraints.
35.	R2H: Rowhammer attack in presence of randomized LLC **G Gaurav, PN Tanksale, VK Tavva** - IEEE 32nd International Conference on High Performance Computing, Data and Analytics Workshop (HiPCW), 2026 **Abstract:** To defend against conflict-based attacks at the Last Level Cache (LLC), randomization is proposed. At the DRAM, to induce the Rowhammer attack, attackers generate memory requests that bypass the on-chip caches and hammer selective DRAM rows. The impact of the set-eviction based Rowhammer attack in the presence of randomized LLC is unexplored till date, and we find it to be ineffective. We propose R2H, a Rowhammer attack that works even with randomized LLC designs. By targeting a subset of cache sets, R2H drives the LLC miss rate comparable to that of conventional caches, in addition these misses are concentrated to specific DRAM rows, enabling a successful Rowhammer attack despite randomized set mappings.
36.	Real-time DEM-based terrain and step farming suitability analysis via geospatial processing in VR **RK Rai,** R Bansal, **SS Jha,** K Yoshida, K Sudo - International Conference on Agriculture-Centric Computation, 2026 **Abstract:** This research presents a novel method that combines geospatial analysis and virtual reality (VR) visualization to evaluate the suitability of mountainous terrains for step farming using Digital Elevation Model (DEM) data. The developed system automatically identifies potential farming zones through slope analysis, transforming raw terrain data into realistic terraced landscapes using discrete elevation quantization. Users can visually explore these results in VR, allowing them to determine the total suitable area for farming and its distribution and to assess farming potential interactively. Initial feedback from users indicates significant Usability and informative value, confirming the practicality and effectiveness of this approach.
37.	Reconfigurable intelligent surface with RS-SAC framework for secure wireless communications **S Bansal, A Sharma** - IEEE Microwaves, Antennas, and Propagation Conference (MAPCON), 2026 **Abstract:** Reconfigurable Intelligent Surfaces (RIS) have emerged as a transformative technology for shaping the wireless propagation environment and enhancing the performance of next-generation communication systems. This paper presents a RIS-assisted framework based on the RS-SAC paradigm, which integrates Rate-Splitting Multiple Access (RSMA) with Sensing and Communication (SAC) to achieve secure and efficient wireless transmission. The RIS plays a central role by dynamically controlling the phase shifts of incident signals, enabling intelligent beamforming that enhances signal quality at authorized users while suppressing leakage to potential eavesdroppers. The proposed RS-SAC framework supports concurrent communication and sensing tasks without compromising security. Simulation results validate the RIS performance of beam steering for sensing the users and beamforming for communication with authorized users. This study underscores the critical role of RIS in enabling secure, intelligent, and multifunctional wireless networks.
38.	Sleep disorder identification using wearable sensors and AI advanced algorithms

	B Kumar… **HA Rizvi,** B Balaji - 5th International Conference on Advancement in Electronics and Communication Engineering (AECE), 2026 **Abstract:** The evidence is increasingly growing according to which early diagnosis and screening of sleep disorders can be affected by the multivariate analysis of the use of nighttime surveillance in combination with wearable technology and machine learning. The prevalence and severity of some sleep disorders including insomnia are on the rise according to the World Health Organisation (WHO) and the medical research hospitals. This dynamic is associated with high levels of daily anxiety, stress, and depressive illnesses. This paper introduces the innovative Internet of Things-based wearable systems architecture to detect sleep issues, and further analyzes this breakthrough of synergy. Our experimental comparisons and comparisons of fair and comprehensive baseline models, such as Bilateral Long Short-Term Memory (BiLSTM), demonstrate the best-performing in the machine learning sphere. The results confirm the outstanding accuracy, precision, and recall of BiLSTM in identifying sleep issues, and, therefore, changing the landscape of healthcare and sleep medical processes. This is a study that, at the intersection point between healthcare and innovation, not only opens the door to the discovery of advanced sleep disorders but also brings another dawn of personalised treatment plans and distance monitoring devices.
39.	Start-of-packet detection: A low-complexity solution for next-gen wireless receivers **S Kaur, A Ahmad, S Agarwal** - National Conference on Communications (NCC), 2026 **Abstract:** This paper presents an interesting and efficient machine learning-based approach for Start-of-Packet (SOP) detection using a proposed Next Generation Packet Detection (NGPD) model. Conventional correlation-based techniques, while simple and effective at high SNRs, tend to degrade significantly in low SNR environments and involve exhaustive computations, making them less suitable for practical or resource-constrained applications. To address these limitations, the NGPD model overcomes the drawbacks of standard SVM in imbalanced SOP detection by employing a class-weighted SVM framework. The model is trained on the received RF signal and evaluated under Additive White Gaussian Noise (AWGN) and Rayleigh fading conditions. Performance is assessed through Probability of Detection, Probability of False Alarm, Mean Absolute Error, and Bit Error Rate. Extensive validation through simulations and hardware experiments using the USRP B-210 confirms that NGPD outperforms both conventional and state-of-the-art methods, achieving an average probability of detection improvement of approximately 2 times over the conventional method, while significantly reducing computational complexity.
40.	Wireless power transfer for polarization-insensitive battery-less IoT beacon **VK Malav,** V Sharma**, A Sharma** - IEEE Microwaves, Antennas, and Propagation Conference (MAPCON), 2026 **Abstract**: This paper presents a microwave-based Wireless Power Transfer (WPT) technique to power polarizationinsensitive and ultra-low-power battery-less Internet of Things Beacon (IoTB). The IoTB includes a compact square patch rectenna with an isosceles triangular-shaped ground, a Power Management Unit (PMU), a Bluetooth Low Energy (BLE) sensor node and a BLE-bridge gateway. The square patch rectenna integrates four Schottky Diodes (SDs) in a conjugately matched manner to achieve maximum power transfer and a two-parallel DC combining network, which is placed perpendicular to each other for achieving full-wave rectification of the incoming Radio Frequency (RF) signals at any orientation. Therefore, the IoTB achieves polarization-insensitivity at any orientation of the incoming wave. The harvested power is delivered to the PMU via rectenna, where a dedicated RF energy transmitter operating in the range of with the transmit RF power of 25 dBm. The IoTB is a well-suited design for deployments of IoT applications that require batteryless and polarization-insensitive features.

41.	You only look at panicles: CBAM-augmented YOLOv8m for precision rice yield estimation from UAV imagery **RK Sanodiya,** S Mondal, P Kumar, RRP Karn - 2026 National Conference on Communications (NCC), 2026 **Abstract:** Accurate detection of rice panicles in aerial imagery plays a critical role in improving yield estimation and precision agriculture. To address this, this paper presents a novel object detection framework based on a customized YOLOv8m architecture augmented with Convolutional Block Attention Modules (CBAM). The proposed approach is trained from scratch on a high-resolution UAV-based rice panicle dataset annotated in YOLO format. To address the challenges of detecting small, densely packed, and occluded panicles, the model enhances feature representation through spatial and channel-wise attention. A comprehensive evaluation has been conducted to assess the model's detection performance under varied real-world field conditions. The results highlight the effectiveness of the attentionenhanced architecture for agricultural monitoring tasks, particularly in scenarios with complex backgrounds and overlapping objects.
C	**Article(s)**
42.	AMCWAVE: Amplitude modulation continuous wave radar for vital estimation **A Hari, R Kumar, B Kumbhani, S Darshi, S Agarwal, JS Sahambi,** S Jain, D Chawla - Measurement: Digitalization, 2026 **Abstract:** Monitoring of vital signs, such as respiration, is crucial for assessing a person's health. Traditionally, contact-based methods have been used for this purpose. Although recent advancements in this field have provided soft, skin-like sensors, and flexible wearable devices have improved comfort, these approaches may still impose certain constraints on continuous monitoring, thereby motivating the development of contactless solutions. To overcome these problems, the recent research focus has been shifted toward contactless monitoring techniques, including camera-based, video-based, and waveform-based methods. In camera and video-based methods, the privacy of the subject is at risk. So, in this study, we propose a radar-based contactless technique named amplitude modulation continuous wave radar for vital estimation (AMCWAVE) for monitoring respiratory signals. This technique involves generating and receiving waveforms using amplitude modulation, which is simpler and less complex compared to alternative approaches. Also, the system model is designed using ADALM-Pluto, MATLAB, and Simulink. The proposed approach is non-contact, remote-operable, cost-effective, less complex, and easily configurable to meet user requirements for respiratory pattern detection. Comprehensive experimental evaluation demonstrates the effectiveness of the proposed method, achieving average root mean square error (RMSE) and mean absolute error (MAE) values of 2.03 and 1.69 breaths per minute (BPM), respectively, along with an average accuracy of 90.00% across all subjects. These results confirm a strong agreement between the estimated and reference respiratory rates under varying conditions. 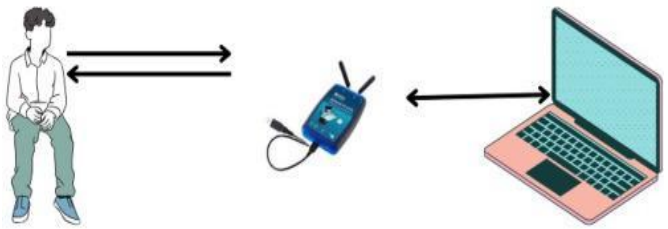
43.	A comprehensive review on development of framework- (MOF/COF/POP) based materials for catalytic conversion of carbon dioxide from dilute/flue gas sources to high-value chemicals **P Rani, CM Nagaraja** - Coordination Chemistry Reviews, 2026

	Abstract: The significant emission of carbon dioxide (CO_2), a primary greenhouse gas, has raised considerable concern about global warming, leading to a worldwide initiative to achieve carbon neutrality. The increase in CO_2 levels has sparked considerable concern about the hazards posed by climate change, severe weather events, and the degradation of wildlife habitats. Consequently, monitoring atmospheric CO_2 levels remains a significant challenge for experts worldwide. Therefore, technologies such as direct air capture (DAC) and integrated conversion are essential. Similarly, direct carbon capture and utilization (CCU) from dilute or flue gas sources is another viable option for CO_2 mitigation. In this regard, highly porous catalytic materials such as metal-organic frameworks (MOFs), covalent organic frameworks (COFs), and porous organic polymers (POPs) exhibit remarkable characteristics, such as tunable porosity, large specific surface areas, highly accessible catalytic sites, and diverse structural and functional properties. These attributes make them exceptional candidates for CO_2 capture from dilute/flue gas sources and the simultaneous transformation of the captured carbon dioxide to valuable chemicals and fuels. This review explores recent advances in framework-based porous materials (MOFs and COFs/POPs), focusing on the chemical conversion of CO_2 from dilute or flue-gas sources into important chemicals and fuels. Furthermore, we outline strategies to enhance the CO_2 (low-concentration) capture and conversion performance of framework materials, the associated challenges, and future perspectives for effective CCU from dilute and flue-gas sources. 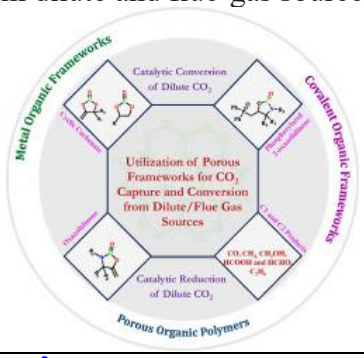
44.	A hybrid finite element-based FE ^{2} formulation for multiscale simulation of heterogeneous materials **S Kumar, N Kumar, M Agrawal** - Computer Methods in Applied Mechanics and Engineering, 2026 **Abstract**: The method is a powerful computational framework for simulating micro-heterogeneous materials while explicitly accounting for microstructural details. However, the conventional displacement-based formulation is susceptible to locking, particularly in thin structural problems or nearly incompressible materials. Capturing the accurate mechanical response in such cases demands extensive refinement of the macroscopic finite element mesh, which, combined with the inherently expensive nested microscale boundary value problems, leads to a dramatic escalation in the computational cost. To alleviate this issue, here, we developed a hybrid element-based formulation in the context of finite deformation. Hybrid formulation deploys hybrid elements based on the two-field Hellinger–Reissner variational principle at macroscale, in conjunction with the second Piola–Kirchhoff stress-based homogenization scheme. Consistency between scales is maintained through the Hill–Mandel condition, and both scales are solved concurrently via a nested Newton–Raphson scheme with appropriate linearizations. The proposed approach is validated through a series of benchmark problems and by comparison with direct numerical simulation (DNS) results. The formulation is also evaluated against the conventional method through various numerical problems, demonstrating its superior computational efficiency.

45.	[A practical approach to transitioning 5G-AKA toward fully and hybrid post-quantum security for 5G and beyond communication] E Choudhary, **AK Yadav,** R Kumar, M Liyanage - IEEE Open Journal of the Communications Society, 2026 **Abstract:** Advancements in 5G are largely driven by its adoption across a variety of applications, including smart homes, smart healthcare, autonomous vehicles, transportation, and Industry 5.0. However, this widespread usage raises significant security and privacy concerns, particularly regarding authentication. To secure 5G communications, 3GPP has standardised the 5G-Authentication and Key Agreement (5G-AKA) protocol. Despite this, state-of-the-art research has revealed that 5G-AKA suffers from several vulnerabilities. In response, numerous alternative authentication schemes have been proposed. Nevertheless, many of these protocols continue to be susceptible to classical security threats, such as malicious serving network (SN) attacks, ephemeral secret leakage, traceability, anonymity violations, and, most critically, a lack of Perfect Forward Secrecy (PFS). Additionally, recent advancements in quantum computing pose a substantial risk to the security of 5G-AKA and its variants, rendering them insecure in the post-quantum era. Although a few post-quantum cryptography-based protocols have been introduced, studies show that they are either computationally expensive or still vulnerable to quantum attacks. In order to tackle these challenges, we propose two versions of a novel authentication protocol that not only provide comprehensive security guarantees but are also computationally efficient. Version 1 utilises a hybrid cryptographic approach (AES + KEM) and achieves the lowest computational cost—even lower than Version 2, which relies solely on KEM. Both versions offer the same level of security, but Version 1 is significantly more efficient in terms of resource usage. We have validated our proposed protocols using the Real-Or-Random (ROR) model and the Scyther tool. Furthermore, we evaluated their performance against existing protocols under both known and unknown attack scenarios. The results show that our protocols incur lower computational, communication, and energy overhead, as well as strong resilience against unknown attacks, outperforming several existing authentication schemes. Furthermore, we implement a testbed to demonstrate the real-time applicability of both proposed versions. 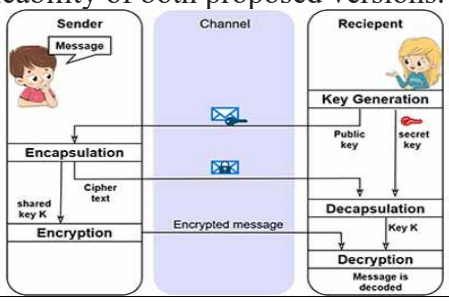
46.	[An adaptive framework for modelling progressive failure in fiber reinforced composites using anisotropic localizing gradient damage model] **A Pandey, S Kumar,** RK Gupta, S Natarajan - Composite Structures, 2026 **Abstract:** This work proposes an adaptive computational framework for modeling progressive intra-laminar failure in transversely isotropic fiber-reinforced composites, with an emphasis on anisotropic damage localization at the mesoscale. The formulation integrates a micromorphic-enhanced, anisotropic localizing gradient damage model, which inherently accommodates evolving nonlocal interactions through a tensorial gradient enhancement. The framework captures directionally dependent fracture phenomena by defining independent internal damage variables for fiber tension/compression, matrix cracking, and shear failure, aligned with the material's orthotropic axes. Nonlocal regularization is enforced through an anisotropic interaction domain, normal to the evolving damage process zone, defined by an orientation-dependent fourth-order

	gradient tensor constructed from the principal stress directions. This mechanism ensures mesh-objectivity and accurate representation of localization phenomena in an anisotropic media. A multi-level adaptive mesh refinement (AMR) algorithm is employed to dynamically resolve damage fronts, driven by equivalent strain and damage based error indicators. The refinement strategy operates hierarchically at the element level, enabling selective refinement in the absence of a priori knowledge of crack paths or initial damage zones. This adaptivity minimizes computational overhead while preserving solution accuracy across multiple scales. The system of coupled governing equations is solved via a numerically stable staggered solution scheme, wherein the displacement and damage fields are updated iteratively using low-order finite elements, ensuring convergence without sacrificing fidelity. The framework is validated against canonical benchmark problems in fracture mechanics, demonstrating quantitative agreement with experimental observations and literature-reported results, thereby confirming the robustness and predictive capability of the proposed anisotropic damage modeling strategy.
47.	Cascading anomaly detection framework in IoT networks **H Anumala -** International Review of Automatic Control, 2025 **Abstract:** Today IoT devices are deployed across multiple business verticals – Healthcare, Transportation. IoT Devices provide vast amounts of data that can be analyzed to provide meaningful insights to end users and organizations. Insights could be recommendations or anomaly detection that can add value to enterprises in terms of energy savings, optimal use of industrial equipment and can avoid fatal system failures. It is crucial to first collect data from heterogenous sensors in standard data formats. Data collection in standard formats is the first step towards applying any Machine learning algorithm. A generic data model is proposed that helps to bridge this gap and translate legacy BACnet and MODBUS sensor data to IoT data formats and also modern IoT data formats including BLE Mesh, LoRA and NB-IoT data to a common model. Also, novel cascading anomaly framework based on a Markov chain is proposed. A Random path algorithm that leverages converged real time data from various IoT devices in various domains including healthcare, automotive and agriculture domains and help provide real time anomaly notifications. The extensive experiment results show that the proposed scheme outperforms the existing state-of-the-art IoT anomaly notification frameworks and help detect early triggers, constructs healthy paths that will avoid fatal states.
48.	Catalytic oxidation of CO from diesel engine exhaust using spinel catalysts (MCo_2O_4) in a ceramic monolith reactor via dip-coating **V Rao Bella,** P Singh, S Trivedi, **T Mondal -** Indian Chemical Engineer, 2026 **Abstract:** In the treatment of automobile exhaust gases, monoliths are the most popular structured reactors, consisting of numerous parallel channels that provide a large open frontal area, ensuring exhaust systems at the end of pipes require a straight gas flow with a very low pressure drop. The outstanding doping qualities and inherent physicochemical properties of spinel-type catalysts have led to their widespread use in automotive exhaust purification. Synthesised cobaltite spinel catalysts (MCo_2O_4, where M = Ni, Co, Cu, Zn) are effectively applied to monolithic carriers using the dip-coating technique, which produces a secondary layer with a greater specific surface area for the best possible dispersion of active species. Characterisation of the catalysts was performed using the XRD, FTIR, SEM, SEM-EDX, TGA, BET and XPS techniques. The adherence test was performed to evaluate the mechanical stability of the catalyst layer and wash-coat. The catalysts were made using the co-precipitation process and then calcined for four hours at 550 °C . The following order describes the catalysts' CO oxidation activity: $NiCo_2O_4 > CoCo_2O_4 > CuCo_2O_4 > ZnCo_2O_4$. To test the stability, the catalysts were heated to 550 °C for 50 hrs, and the catalysts showed satisfactory thermal stability.

	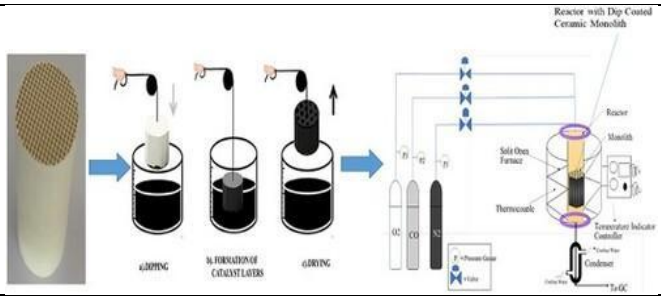
49.	CBAR: A Cooperative Buffer-Aware Routing using node reliability for opportunistic IoT networks **A Phutela, S Pal,** S Sampalli - Ad Hoc Networks, 2026 **Abstract:** Opportunistic networks (OppNets) provide a flexible communication paradigm in environments where traditional infrastructure fails or unavailable, such as smart cities and IoT-enabled mobile systems. The challenging aspect of these networks remains efficient routing due to high node mobility, limited buffer capacity, and intermittent connectivity. The dependence on opportunistic node encounters makes efficient routing a critical challenge. In this work, an attempt has been made to address these issues. CBAR (Cooperative Buffer-Aware Routing), a message forwarding scheme designed for Opportunistic IoT Networks (OppNets), is proposed. This work leverages cooperative behavior among nodes and reliable forwarders based on encounter history and delivery performance, which are identified by their Reliability Index (RI). A Drop Message Index is used to retain messages with higher delivery potential while discarding those prone to expiration or excessive delay to optimize the limited buffer resources. An acknowledgment is used to minimize redundant transmissions. The simulation results of the proposed algorithm demonstrate that CBAR achieves 39.24% higher delivery ratio compared to UCbR and preserves 27.98% more energy compared to UCbR. Additionally, CBAR reduces the average delay by 13.37% and routing overhead by 43.29% with FCR. The results obtained highlight the effectiveness of CBAR in improving reliability, resource efficiency, and cooperative communication in OppNets.
50.	Characterizing optimal monitoring edge-geodetic sets for some structured graph classes F Foucaud, **A Pandey, K Paul** - Discrete Applied Mathematics, 2026 **Abstract:** Given a graph G=(V,E), a set S⊆V is said to be a monitoring edge-geodetic set if the deletion of any edge in the graph results in a change in the distance between at least one pair of vertices in S. The minimum size of such a set in G is called the monitoring edge-geodetic number of G. In this work, we provide structural characterizations of the minimum monitoring edge-geodetic sets for several structured graph classes: distance-hereditary graphs, P_4-sparse graphs, bipartite permutation graphs, and strongly chordal graphs. These characterizations are in terms of the mandatory vertices of the graph (those that need to be in every solution). This extends previous results from the literature for cographs, interval graphs and block graphs, and leads to efficient algorithms to compute optimal monitoring edge-geodetic sets for graphs in these graph classes.
51.	Computational study of aerodynamic characteristics in flapping MAVs at different angles of attack **R Kumar, SS Padhee, D Samanta** - Sadhana Academy Proceedings in Engineering Sciences, 2026 **Abstract**: In this study, we conducted numerical simulations of a rectangular wing's flapping motion within a three-dimensional flow field using the discrete vortex method (DVM). This method is more computationally efficient because it avoids the need for generating a flow field grid at each time step, unlike the traditional simulation techniques. We evaluated the wing's aerodynamic performance by measuring the lift and drag. The wing was subjected to a combination

	of chord-wise twisting and span-wise bending at varying angles of attack. In addition, a prescribed motion was imposed on the flapping wing motion. Our findings indicate that the deformable wing produces significantly more lift than a rigid wing, with only a slight increase in drag. Consequently, the lift-to-drag ratio demonstrates that deformable wings are more efficient at generating lift within a moderate angle of attack range, typically between 10 and 20. A numerical model is employed to capture the basic wake shape and to account for more complex fluidic phenomena, such as vortex stretching. The insights from our numerical simulations are expected to provide a valuable direction for modeling the micro-air vehicles (MAVs).
52.	Correlation of size, structure and thermodynamics of alloying additions on β-phase stabilization in Ti alloys **K Kumar, A Verma, H Singh,** K Guruvidyathri, **K Rakha** - Modelling and Simulation in Materials Science and Engineering, 2026 **Abstract:** Novel *β*-Ti alloy development through advanced manufacturing technologies like additive manufacturing (AM) requires a robust understanding of the effect of alloying additions, especially on the martensite transformation behavior. Avoiding martensite is the other side of the same coin as stabilizing *β*-phase in rapid cooling is associated with such processes. In this study, for the individual binary combinations of the alloying elements with Ti, the calculated and experimental martensite start temperatures () are comprehensively analyzed for the atomic radii and crystal structure effects, in the light of latest Calphad (Calculation of Phase Diagram) data. Wherever not available, thermodynamic database files were compiled in-house. Important trends are revealed with regard to the atomic radii within a type of crystal structure of alloying additions on martensite transformation. For a specific crystal structure, a trend of decreasing solute composition limit for martensitic transformation with increasing atomic size difference between the alloying element and Ti is seen. Effect of atomic size difference between solute and solvent on distortion in the product phase, vis-à-vis on the strain energy barrier for martensitic transformation, and *β*-phase stabilization are discussed. The study provides useful insights for the selection of alloying elements while designing Ti alloy for processes such as AM. The results are validated using experiments on one selected alloy, i.e. Mo addition to Ti, since Mo is identified as non-toxic and allergy free *β*-phase stabilizer to Titanium for biological application. The microstructural and phase analysis using optical microscopy, energy-dispersive x-ray spectroscopy, and x-ray diffraction of as-cast and homogenized Ti-Mo alloy match with the revealed theoretical trends.
53.	Coupled effects of viscosity contrast and phase separation in hydrodynamically stable radial hele-shaw flow P Verma…**M Mishra,** CY Chen - Journal of Fluid Mechanics, 2026 **Abstract:** We investigate a nonlinear interaction between viscous fingering (VF) and phase separation (PS) in a binary fluid system within a radial Hele-Shaw cell. Through nonlinear simulations, we analyse displacement under favourable viscosity contrast, in which a more viscous fluid displaces a less viscous one, and PS may induce VF. The system undergoes PS when the concentration lies within the spinodal region, where the second derivative of free energy is negative. In the absence of viscosity contrast, the flow exhibits distinct morphologies, rings under the strongest PS conditions and droplets otherwise. A distinct composition of separated droplets results from uphill and downhill diffusion imbalances. The prominence of PS is characterised by the interfacial tension within the spinodal region, while the extent of pattern rupture is quantified by the interfacial length in the fully separated region. We identify interfacial tension as a reliable and experimentally accessible indicator of PS. It offers a practical alternative to the second derivative of free energy, which is challenging to quantify directly. We find that higher miscibility stabilises the overall pattern, as evidenced by reductions in both interfacial tension and interfacial length. In contrast, viscosity contrast plays a complex role: while a favourable viscosity contrast

	generally stabilises the flow by reducing interfacial length, there are specific flow conditions under which the interfacial length increases despite a weaker PS condition. Our results reveal instability patterns consistent with experimental observations, reinforcing the reliability of our findings. 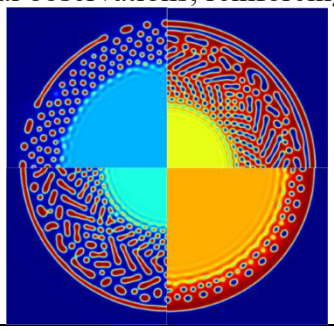
54.	Cu 2 O@ COF core–shell catalyst for electrochemical CO 2 reduction W Tahir, E Liberra, IE Khalil, **P Das**…Arne Thomas - Journal of Materials Chemistry A, 2026 **Abstract:** The electrochemical reduction of CO_2 (CO_2RR) to C_{2+} products offers a sustainable approach for carbon utilization and the production of valuable chemicals. Cu_2O nanocubes (NCs) have emerged as effective electrocatalysts for the formation of C_{2+} products. In this study, we applied a coating of Cu_2O NCs with robust covalent organic framework (COF) layers prepared by multicomponent reactions. Compact layers of COFs are formed, which, due to their porosity, allow full accessibility of the Cu_2O catalytic surfaces to CO_2 molecules. Furthermore, the thickness and chemical functionality of the COF layers can be continuously varied by changing the type and quantity of monomers used to cover the Cu_2O NCs. Electrocatalytic measurements demonstrate that these hybrid core–shell Cu@COF systems remain active in CO_2 reduction, achieving good current density and faradaic efficiency, while maintaining selectivity for the desired CO_2 reduction products. Additionally, the COF shell provides remarkable stability to the system under electrochemical conditions.
55.	Cyclic reformation of subcritical perpendicular fast magnetosonic shocks due to oblique whistler waves ME Dieckmann, **L Palodhi**… R Walder - New Journal of Physics, 2026 **Abstract:** The stability of subcritical perpendicular fast magnetosonic (FMS) shocks, which are propagating at 1.7 times the FMS speed, is investigated using two-dimensional particle-in-cell simulations. The plasma, composed of electrons and fully ionized nitrogen, is permeated by a uniform magnetic field oriented at 45° to the simulation plane normal. This configuration results in a diamagnetic current that sustains the shock's magnetic ramp and is partially resolved within the simulation plane. The diamagnetic current drives an oblique lower-hybrid gradient drift instability within the ramp. This instability has been observed in magnetic reconnection experiments and studied in the framework of a Harris-type sheath in previous studies. It arises from a reactive coupling between the oblique Whistler wave, which is propagating backward in the electron rest frame, and the forward-propagating ion acoustic wave. Our simulations show that the magnetic component of this wave modulates the shock's magnetic field, while the electrostatic ion density modulation forces the shock to collapse into a magnetic piston and then reform. The reformation is not forced by an external perturbation as in previous simulations but by the oblique Whistler wave.
56.	Developing a subject/research guide for academic libraries: A case of IIT Ropar Library **H Kaur,** G Singh, **DK Siddaiah** - Library Hi Tech News, 2026 **Abstract:** Purpose: This case study aims to explain how a library at a higher education institution developed a subject/research guide using the SubjectPlus tool to enhance library usage. It also

	provides the academic disciplines for which subject/research guides have been created. Design/methodology/approach: This paper uses the case study approach to analyse how the SubjectPlus tool is used to develop subject/research guides. The study evaluates past practices for finding resources and how the utilisation of modern tool changed the user experience. Findings: The Library of IIT Ropar developed the subject/research guides powered by SubjectPlus, which is now successfully deployed. This tool is identified as one of the most beneficial for academicians and researchers, providing on- and off-campus access. Users can access subject- and topic-specific print and online resources via the A-Z list or subject-wise, and enjoy many other features. Originality/value: This paper assists library professionals in understanding the development of subject/research guides and how users at higher education institutions effectively use library resources. With the help of the SubjectPlus tool, users can have access to key information resources related to a particular academic subject or field of study.
57.	Direct measurement of the 7Li(p,α)4He reaction at astrophysical energies using the ELISSA array H Pai…**R Roy**… N Vukman - Physical Review C, 2026 **Abstract**: A direct measurement of the 7Li(p,α)4He reaction at astrophysical energies was performed at the Horia Hulubei National Institute for R&D in Physics and Nuclear Engineering (IFIN-HH) using a scaled-down version of the ELISSA detector array and the 3 MV Tandem accelerator. This reaction plays a crucial role in both primordial and stellar nucleosynthesis. In Big-Bang Nucleosynthesis (BBN), it is directly linked to the long-standing "Cosmological Lithium Problem," the discrepancy between observed and predicted primordial 7Li abundances. In stellar environments, it constitutes the final step in the hydrogen-to-helium burning chain. The experiment utilized a 7Li beam incident on a CH2 target at ten laboratory energies (Elab) corresponding to center-of-mass energies (Ec.m.) ranging from 59.5 to 990 keV. The astrophysical S factors were extracted using both the Distorted Wave Born Approximation (DWBA) and polynomial fitting techniques. Updated reaction rates were calculated from the present DWBA results, supplemented by existing experimental data. The impact of the theoretical DWBA calculation on the reaction rate is investigated.
58.	Dynamics of an internally actuated weakly elastic sphere in a general quadratic flow **S Verma, NK Marath** - Soft Matter, 2026 **Abstract:** Internally actuated elastic particles are widely used in biomedical applications. It is imperative to understand the dynamics of such particles in pressure-driven microfluidic devices to manipulate their motion. We analytically examine the dynamics of an internally actuated elastic particle translating in a general unbounded quadratic flow in the inertialess limit. We consider the particle as a compressible weakly elastic sphere, and its motion is controlled by applying an external point force and a point torque at the centre of its undeformed shape. The fluid and the particle are modelled using the Stokes and the Navier elasticity equations, respectively. We use the domain perturbation method to capture the particle deformation. The point force and the point torque are obtained until $O(\alpha^2)$, assuming $\alpha \ll 1$. Here, α is the measure of the particle elastic strain induced due to the fluid viscous stress. First, we present the results for the particle motion in a general unbounded quadratic flow. The results are simplified further for the motion along the centreline in the quadratic component of three Poiseuille flows: (1) elliptical Poiseuille, (2) plane Poiseuille, and (3) Hagen–Poiseuille flows. In the general quadratic flow, the point force at $O(\alpha)$ is aligned with the particle velocity, while the force at $O(\alpha^2)$ acts at an angle to the velocity. Furthermore, the torque is non-zero due to elastic effects at $O(\alpha)$ and $O(\alpha^2)$. For all the three Poiseuille flows, the point force until $O(\alpha^2)$ is aligned with the particle velocity, while the torque is zero.

59.

Efficient molecular solar thermal energy storage in self-assembled columnar triethynylbenzene-Azobenzene systems

R Talukdar, Ashy, Kiran, Shreya, M Gupta - Chemical Communications, 2026

Abstract: A self-assembled columnar hexagonal liquid crystal based on tetra-ortho-fluoro azobenzene-functionalized triethynylbenzene is reported for molecular solar thermal energy storage. Efficient visible-light-driven E→Z photoisomerization (~80%) at ambient temperature and significant heat release (up to 12.3 °C) upon back-isomerization demonstrate its potential as an effective MOST material.

60.

Electrochemical divergent synthesis of azetidines via strain release of 1-azabicyclo [1.1. 0] butanes

N Duhan, S Dutt, SK Rastogi, P Banerjee - Angewandte Chemie International Edition, 2026

Abstract: Due to the favorable pharmaceutical properties of the azetidine ring, it can serve as a bioisostere to replace saturated heterocycles such as piperazines, piperidines, and pyrrolidines in drug discovery. The diverse methods for azetidine synthesis are still limited and challenging. Herein, we design a new class of 1-azabicyclo[1.1.0]butanes (ABBs) and report the first electrochemical protocol for the synthesis of chemo-selective trifluoromethanesulfonylated and trifluoromethylated azetidine derivatives via direct anodic oxidation. The key features of this strategy involve: (i) electrochemical anodic oxidation of ABB to form a *N*-centered radical cation, (ii) a rare [2,3]-sigmatropic shift of sulfone, (iii) selective oxidation of Langlois' reagent ($NaSO_2CF_3$), and (iv) the kinetic study of the developed methodology. The strategy exhibits broad substrate scope and scalability, making it practical. Installation of generated azetidines into marketed drug motifs, including ibuprofen, naproxen, and olaparib derivative, demonstrates the method's utility. Mechanistic investigations, supported by control experiments, cyclic voltammetry, and electrochemical impedance spectroscopy (EIS), provided key insights into the reaction pathway. This electrochemical approach advances the strain-release chemistry of ABBs and offers a promising platform for future developments.

A new class of 1-azabicyclo[1.1.0]butanes (ABBs) is synthesized, and the first electrochemical method for synthesizing chemo-selective trifluoromethanesulfonylated and trifluoromethylated azetidine derivatives from ABBs. This strategy involves the anodic oxidation of ABB to generate a nitrogen-centered radical cation, a rare [2, 3]-sigmatropic shift of the sulfone, and selective oxidation of Langlois' reagent. The generated azetidines were integrated into drug motifs, demonstrating their utility. Mechanistic investigations through control experiments, cyclic voltammetry, and electrochemical impedance spectroscopy (EIS) provided deep insights into the reaction pathways.

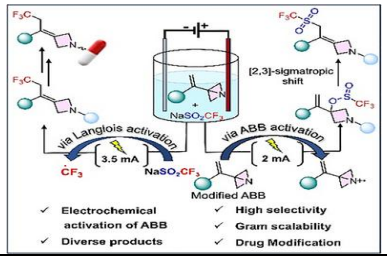

61.

Electroreductive cross-coupling of cyclopropyl ketones and aryl methyl ketones to access 1, 2, 4-triarylbenzenes via acid-promoted aromatization

R Bag, C Laru, D Saha, R Banerjee, P Banerjee - Organic Letters, 2026

Abstract: Herein, we report an electroreductive radical–radical cross-coupling between radical intermediates generated from the reduction of cyclopropyl ketones and the aryl methyl ketones, furnishing a *δ*-hydroxy ketone intermediate that undergoes acid-promoted aromatization to afford 1,2,4-triarylbenzenes. This telescopic two-step synthetic strategy obviates the need for external

	oxidants or reductants and provides a broad substrate scope with remarkable functional group tolerance. Additionally, the practicality of the designed strategy was evidenced by its scalabilityand further derivatization of the synthesized triarylbenzenes. 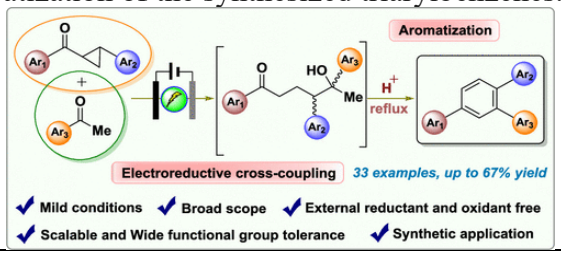
62.	Electroreductive deconstruction and oxygenation of cyclic amines **S Dutt, N Duhan, V Kale, P Banerjee** - Green Chemistry, 2026 **Abstract:** Here, we introduce a greener, atom-economical, and sustainable electroreductive deconstructive functionalization approach (E-Factor = 0.9) for transforming cyclic amines into δ-substituted amides via C-N bond cleavage, and further extended towards the synthesis of δ-ketoamides through the trapping of environmentally benign oxygen molecules without using any sacrificial hydrogen donor, oxidant/reductant, or catalyst. Several structurally modified cyclic amines, ranging from strained to unstrained ring systems, were employed to synthesize corresponding structural moieties that are difficult to construct through traditional methods. Late-stage derivatization of proline incorporating natural and medicinally active compounds has also been performed. Moreover, we conducted electrochemical scaffold hopping of a bridged bicyclic amine to generate γ-lactone. Remarkably, our strategy proved scalable, and further derivatization of our product has been carried out to demonstrate its synthetic utility. A detailed mechanistic study has been performed to understand the reaction pathway. 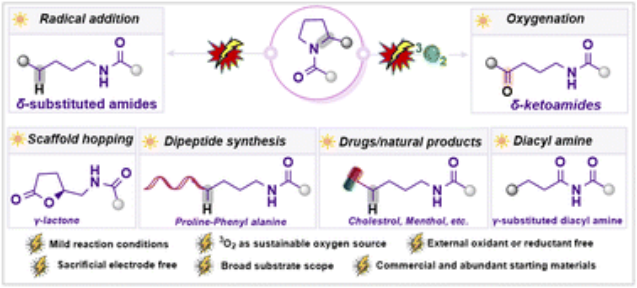
63.	Emerging technology forecasting for the VHF data exchange system in maritime wireless communication M Woo… **A Nanda** - Journal of Marine Science and Technology, 2026 **Abstract:** The VHF Data Exchange System (VDES) is emerging as a critical standard in maritime communication to overcome the capacity and protocol limitations of the legacy Automatic Identification System (AIS). As VDES enters a pivotal phase of international standardization, identifying strategic R&D priorities and undeveloped technological areas is essential. This study proposes a systematic forecasting framework by integrating Latent Dirichlet Allocation (LDA) and Generative Topographic Mapping (GTM) to analyze the VDES patent landscape. Through LDA, we identified four primary technological domains of VDES: (1) cloud and edge computing-based traffic management system, (2) satellite–terrestrial interconnected bidirectional wireless communication network, (3) high-reliability encryption-based security system, and (4) bidirectional communication system through data modulation module. Subsequent GTM analysis identifies technological vacuums specifically within the cloud and edge computing-based traffic management system and the bidirectional communication system through data modulation module. Our findings show that connectivity and security frameworks are relatively mature while

	intelligence-centric operational optimization remains underexplored. This study provides empirical evidence to guide future R&D directions in maritime data exchange systems.
64.	Enhanced electron–phonon coupling due to layered-perovskites octahedral tilting in hole doped cuprate superconductor Isha, D Singh…**R Ahuja**…AK Yogi - Journal of Physics - Condensed Matter, 2026 **Abstract:** The electron–phonon (e–ph) coupling is crucial in explaining various ordering phenomena such as superconductivity and charge density waves (CDWs) which has been invoked to explain Cooper pair formation leading to superconductivity, however, the origin of charge state mechanism is not yet fully understood. Here we study the role of e–ph coupling in understanding the interplay of the structural phase transition, CDW transition, superconducting transition, and flat electronic band dispersion in the LaSrxCuO$_4$ (x = 0.15) superconductor. We employed high-resolution temperature dependent x-ray diffraction and Raman scattering measurements in combination with first-principles calculations across the phase-transitions. We unveil the dominant role of CuO$_6$ octahedra distortion and tilting which suggests the presence of strong e–ph coupling that gradually develops high alternating CuO$_6$ octahedra rotations [in-phase (+ve) and anti-phase (–ve); 3°)] which can further enhanced e–ph coupling below the structural-phase transition (= 150 K), leading to the symmetry-breaking. We observe that the local distortion of CuO$_6$ including tilting and phonon modes at 430, 360, 225, and 100 cm^{-1} may associated with CDW correlations below . Further, our theoretical calculations across the superconducting transition suggests the presence of strong hybridization of Cu 3d with O 2p orbitals, indicating the role of alternating CuO$_6$ octahedra tilt in the electronic structure of LaSrxCuO$_4$. Thus, the octahedral tilt played a crucial role in the origin of the CDW phase.
65.	Enhancing network traffic classification with autoencoders and TF-IDF-based dimensionality reduction: A data-centric comparative study **S Mishra** - Computer Networks, 2026 **Abstract:** Traditional traffic classification techniques, such as port-based methods and Deep Packet Inspection (DPI), are increasingly ineffective due to encryption, dynamic port usage, and dependency on network-specific settings. Existing AI-based solutions also struggle with issues like overfitting and poor generalization caused by inadequate feature selection, leading to degraded service quality and undetected anomalies. To address these limitations, we introduce Corelith, a novel hybrid model combining autoencoders with an XGB classifier (payload-based data-centric approach). Leveraging TF–IDF vectorization for preprocessing, Corelith reduces feature sparsity to **14.45%**, enabling efficient dimensionality reduction and achieving a **57.14%** reduction in storage requirements. Unlike traditional models that rely on full feature sets, Corelith maintains high accuracy (**97.50%**) using a reduced-dimensional input, matching supervised model performance while outperforming unsupervised methods. Tested in Mininet orchestration and real-world deployments, Corelith accurately identifies abnormal traffic, labels captured packets, and guides resource allocation. Its ability to pinpoint secure paths and optimize frequency use demonstrates the transformative potential of lightweight, hybrid AI models in enhancing network performance, scalability, and security.
66.	Experimental investigation on characterization of solid soot particle emissions using in-situ developed thermal desorption system from reactivity-controlled compression ignition engine **S Rana, MR Saxena, RK Maurya** - Journal of Traffic and Transportation Engineering (English Edition), 2026 **Abstract:** This study experimentally investigates the solid soot particle number emissions from the gasoline-diesel (GD) and CNG-diesel reactivity-controlled compression ignition (RCCI) engines. The volatile organic fraction should be removed from the sampling gas before particle

	measurement to analyze the correct number of solid particle emissions. In the present study, a thermodesorption system is developed to remove the volatile particles from the exhaust sample. This study examines the effect of the thermodesorption system on emissions of nanoparticles from the RCCI engine. The intake manifold of the diesel engine is modified to inject gasoline/CNG to run an engine in RCCI mode. The experiments are performed at different fuel premixing ratios (r_p). The fuel is varied by changing the port-injected gasoline/CNG mass. A differential mobility spectrometer has been used to measure the emissions of nanoparticles. The thermophoresis and diffusion particle losses in the thermo-desorption system are estimated. It is found that the diffusion losses are 4.7%, 2.0%, 1.0%, and 0.2% for 10, 30, 50, and 100 nm diameter particles, respectively, whereas the thermophoresis losses are 7.6% for the same particle diameter. The results depict that the developed thermodesorption system can remove volatile particles with high volatile particle removal efficiency. Nucleation mode particles (NMPs) are significantly reduced with the thermodesorption system. The peak of the NMPs in the 10–30 nm size range is reduced by an order of magnitude when sampling is performed with the developed thermo-desorption system at all premixing ratios for gasoline-diesel and CNG-diesel RCCI combustion.
67.	Exploring tonal contrasts in Dharamshala Tibetan using mathematical modeling, statistical modeling, and machine learning algorithms **S Sarkar, S Kar,** A Gope - Language and Linguistics, 2026 **Abstract:** This paper examines the tonal system of Dharamshala Tibetan (DT) through a comprehensive phonetic and phonological analysis, employing statistical tests, regression modeling, mathematical modeling, and machine learning algorithms (MLAs). Our aim has been to determine the number and nature of tonal contrasts in DT, an issue that remains unresolved to date. The stimuli (tonemes), consisting of two-way and three-way meaning contrasts, are designed based on preliminary fieldwork and consultations with native speakers. Acoustic analyses reveal three distinct tonal categories supported by significant differences in fundamental frequency (f0), including f0 height and f0 directionality, duration, and intensity. Although initial f0 data analysis, particularly f0 directionality, suggested rising contours, further analysis confirmed these as (i) two level tones, *viz*. high (H) and low (L), and (ii) one contour tone, *viz.*, mid-rising (MR), with consistent pitch trajectories. MLAs were employed to classify the tones, with confusion matrices highlighting the prominence of misclassifications involving mid-rising tones. This supports the hypothesis that the mid-rising tone may be a recently emerged category. The findings of this work are contextualized within the broader framework of Tibetan phonology, providing valuable insights into the tonal characteristics of DT. This study underscores the importance of integrating quantitative approaches with linguistic theory to deepen our understanding of tonal systems.
68.	Extraction of aggregation kernel from DEM simulations for granulation in presence of sustained contacts A Karar…**J Kumar,** A Tripathi - Chemical Engineering Science, 2026 **Abstract:** Granulation is a popular size enlargement process, typically modeled using the population balance model (PBM). PBM requires the knowledge of breakage, aggregation, growth and nucleation kernels. While discrete element method (DEM) offers an alternative to phenomenological models for kernel extraction, existing models predominantly rely on relative velocity, specifically, the collisional velocity between particle pairs, neglecting the role of sustained contacts and the resulting evolution of liquid/solid bridge. In this work, we demonstrate a new method to extract aggregation kernels as a time snapshot by analyzing the particle locations over a certain number of time steps around that particular time. We propose a series of physically grounded criteria to determine aggregation efficiency using detailed information of the contact duration, relative overlap and the number of attachments/detachments. Finally, the obtained information is translated in the form of aggregation kernel by using appropriate expressions. This

	contact information-based kernel extraction methodology is validated successfully by reproducing well-established kernels, such as Brownian kernel and gravitational settling kernel. The approach is then applied to extract aggregation kernels for rotating drum and fluidized bed granulation systems involving wet particles, demonstrating its applicability to real-world scenarios.
69.	Failure mechanics of carbon nanotube modified epoxy adhesives in co-cured composite T-joints: Experimentally informed cohesive zone modelling **S Bansal, PK Agnihotri** - Engineering Failure Analysis, 2026 **Abstract:** Improving the strength and toughness of composite T-joints is important to ensure their integrity in structural applications. Present study demonstrates how the addition of carbon nanotubes (CNTs) in pure epoxy adhesives (PA) improve the load bearing capability of co-cured composite T-joints. Experiments show that the strength and toughness of PA adhesive increase significantly in CNT modified epoxy adhesives (CMA). Both these parameters improve by 53 % and 50 % in opening/normal mode and 29 % and 36 % in sliding/tangential mode respectively. The opening and sliding mode traction separation laws (TSLs) are determined from the test data for cohesive modelling of PA and CMA adhesives. The comparative analysis reveals that T-joints prepared with CMA exhibit better integrity than those prepared with PA. The strength and toughness of CMA T-joints increase by approximately 49 % and 203 %. The strengthening of epoxy, better resistance against sliding, and higher essential work of fracture (EWF) of CMA adhesives are primarily responsible for the better integrity in CMA T-joints. Fractography analysis reveal that CNT pullout and cusp formation are the dominant fracture mechanisms that lead to higher strength and toughness in CMA T-joints. Finally, it is shown that the addition of CNTs increases strength, essential work of fracture and induces addition energy dissipating mechanisms in pure epoxy adhesives and thereby enhances the integrity of co-cured composite T-joints.
70.	FedHC: Enhanced federated learning with Hessian and cosine correlation for proximal correlation KP Singh…**SK Vipparthi, GSR Kosuru,** S Murala, MA Mottaleb - Knowledge-Based Systems, 2026 **Abstract:** Federated Learning (FL), a prominent distributed learning approach, involves both collaborative and individual data updates from participants. FL faces a key challenge with heterogeneous data causing local drift. Conventional methods like FedDC, relying on first-order optimization techniques such as Stochastic Gradient Descent (SGD), struggle to address this effectively. These techniques are not fully effective in mitigating local drift or ensuring optimal convergence. There is a growing interest in second-order optimization methods for better convergence. Yet, these advanced methods introduce distinct convergence challenges within the FL framework. To address these challenges, we propose a novel FL method called FedHC. The proposed FedHC integrates proximal correction within the objective function and employs an approximated Hessian optimizer for updating local model parameters. Experimental results, conducted on diverse image classification and synthetic datasets, show that FedHC significantly improves convergence speed and outperforms existing methods, demonstrating robustness across different client settings.
71.	Finite element method for interaction of oblique surface waves with dual vertical barriers over arbitrary bottom N Kumar, **SC Martha** - The Anziam Journal, 2026 **Abstract:** Within the framework of small-amplitude water wave theory, the scattering of obliquely incident monochromatic surface waves by dual thick vertical barriers over an arbitrary bottom topography is analysed. A numerical model based on the finite element method is developed by formulating the governing well-posed mixed boundary value problem over each element within a truncated finite domain. This domain is obtained by limiting the originally infinite domain to a

	finite distance. Two types of bottom profiles, namely parabolic and rectangular, are considered for the numerical analysis. To ensure the accuracy of the present numerical results, an energy identity relation is derived using Green's identity and verified numerically. Additionally, for validation purposes, the numerical results are compared with existing results available in the literature. The number of zeros on the reflection and transmission coefficient curves is investigated with respect to the gap between identical and nonidentical barriers. The effects of various physical parameters, including the gap between the vertical barriers, the height of the bottom topography, the thickness and length of the barriers, and the angle of wave incidence on the reflection and transmission coefficients, as well as on the nondimensional horizontal force acting on the front and rear barriers, are examined using the proposed numerical model. This study contributes to understanding of wave–structure interaction and will be useful in addressing similar problems in applied mathematics and fluid mechanics.
72.	Finite-temperature phase diagram and collective modes of coherently coupled bose mixtures V Sunilkumar, **Rajat, S Gautam,** A Roy - Physical Review A, 2026 **Abstract:** We investigate the ferromagnetic-paramagnetic phase transition in coherently (Rabi-)coupled Bose-Einstein condensates at zero and finite temperatures, exploring different routes to the transition by tuning the Rabi coupling or increasing the temperature at a fixed coupling. Using the Hartree-Fock-Bogoliubov theory within the Popov approximation, we map out the finite-temperature phase diagram of a three-dimensional homogeneous condensate. The critical line is identified from the softening of the spin gap, which at finite temperature does not strictly close but exhibits a discernible minimum. Magnetization and the spin dispersion branch reveal the progressive suppression of the ferromagnetic order with increasing temperature. In quasi-one-dimensional harmonic traps, the transition, driven by Rabi coupling, does not correspond to a sharply defined critical point. To this end, we use the softening of the spin breathing mode as an operational indicator of the transition, whose minimum shifts to lower coupling strengths with increasing temperature. Notably, the thermally driven transition causes monotonic hardening of all the spin modes. For both coupling and the temperature-driven transition, the hybridized "density" modes in the ferromagnetic phase acquire more density character while approaching the critical point.
73.	Grain-refinement-mediated tribo-oxidation and corrosion trade-offs in a dual-phase AlCoCrFeNi high-entropy alloy **D Singh,** SK Sharma, MK Mishra, **R Kumar** - Tribology International, 2026 **Abstract:** This present work examines how grain refinement influences wear mechanisms and corrosion behaviour in a dual-phase $Al_{1.5}Co_{0.5}CrFe_{1.3}Ni_{2.2}$ high-entropy alloy (HEA) processed by ball milling and spark plasma sintering. Grain refinement altered the phase distribution and strengthened the alloy through grain-boundary effects. It resulted in a significant reduction in the specific wear rate for the ultrafine-grained (UFG) HEA, despite containing a lower BCC fraction. The coarse-grained (CG) HEA exhibited severe abrasive wear with wider and deeper grooves. In contrast, the UFG alloy showed mixed abrasive-oxidative wear, with narrower wear tracks and tribo-oxide layers. Electrochemical testing in 3.5 wt% NaCl revealed an opposing effect of grain refinement on corrosion performance, with the CG HEA exhibiting superior corrosion resistance due to the formation of a stable Cr-rich passive film. In contrast, a thinner Al-rich oxide layer formed on UFG HEA, and micro-galvanic interactions intensified between the FCC and BCC phases, resulting in accelerated corrosion. The results demonstrate the role of grain refinement in modifying the tribo-oxidation and corrosion mechanisms in dual-phase HEA, reflecting a clear trade-off between wear resistance and corrosion stability. These findings provide insight into microstructural design strategies for balancing competing degradation mechanisms in multiphase HEA.

74.	Impact of isolated shallow rocking foundation on fragility of RC shear wall structure **RM Kannan, P Haldar, N James** - Structures, 2026 **Abstract:** Devastating consequences of RC-framed structures with shear walls under seismic excitation have stirred up concern regarding understanding nonlinear behavior and ensuring seismic safety of shear walled RC framed structures, one of the most preferred structural systems for multistorey buildings. This study concentrates on the effects of the rocking foundation, which is systematically underproportioned to uplift and takes advantage of the inelasticity of the underlying soil. Seismic response of a two-dimensional shear wall frame system with rocking foundation has been compared with the conventionally designed rigid ones. Seismic responses and associated damage probability assessment have been conducted using a series of nonlinear time history analyses and fragility analyses, respectively for varying soil typologies. It has been observed that conventionally designed footings experience the highest seismic-induced moments, which can be reduced by up to 50%, by allowing slight and moderate rocking of the footings. However, foundation rocking increases the settlement at foundation level and roof displacements than the conventionally designed ones. This observation indicates that allowing foundation rocking decreases the force demands with increasing displacement demands. Based on the observations from this study, it can be concluded that reducing the design moment factor up to 0.87 for medium dense sand, 0.78 for dense sand and 0.70 for very dense sand is beneficial for enhancing the overall performance of RC shear wall structure. This study also indicates that the overdesigned footing may not always be beneficial for super structure.
75.	Inductance measurement technique for switched reluctance motor using SPWM and a cascaded-second order generalized integrator **Z Rayeen, A Azeem**, A Iqbal, **S Payami** - IEEE Transactions on Instrumentation and Measurement, 2026 **Abstract:** The winding inductance of an electric motor is one of the most critical parameter for evaluating its performance. In switched reluctance motors (SRMs), the winding inductance dynamically changes with rotor position and phase current, posing significant challenges for its measurement. In literature, the conventional AC methods utilized for inductance measurement neglect core saturation. The core saturation leads to detrimental effect such as waveform distortion and thereby compromise inductance measurement accuracy, when ignored. Thus, this article proposes a novel strategy to measure the winding inductance of five phase outer rotor SRMs (OR-FPSRM) at varying excitation current and rotor positions. The proposed method is articulated by utilizing the concept of simple sinusoidal pulse width modulation (SPWM) switching scheme. In this method, the OR-FPSRM is excited through asymmetric converter utilizing SPWM switching scheme at standstill condition to estimate the winding inductance via injection of a sinusoidal as a fundamental frequency component. This method employs a cascaded second-order generalized integrator (C-SOGI) to mitigate distortion caused by core saturation. Additionally, the C-SOGI filter is precisely tuned to attenuate the DC component, eliminating errors from noise and inherent DC offset in sensor signals. Thus, the proposed work introduces a low cost simplified approach that enhances the accuracy of inductance measurement eliminating the requirement of additional devices, such as power analyzers or true RMS meters which incurs high cost. The finite element analysis (FEA) to investigate proposed work is carried out with the ANSYS Maxwell simulation environment. The experimental prototype of OR-FPSRM motor rated at 3kW is utilized to validate the proposed work.
76.	Influence of dielectric properties on electrical discharge machining process using EDM oil vs. graphite mixed EDM oil S Kalakonda, PS Rao, **R Kant** - Results in Surfaces and Interfaces, 2026

	Abstract: Dielectric properties play a very important role in the electro-discharge machining process. The reason behind this is that adding powder granules to the dielectric improves a more conductive environment, which in turn increases sparking between the tool and the workpiece. In this research, two stages of testing was done, First stage initial dielectric testing of both dielectrics, Electro Discharge Machining oil (EDM oil) and Graphite Mixed Electro Discharge Machining oil (G.M EDM oil) to determine dielectric properties of both oils such as breakdown voltage (BDV), thermal conductivity, viscosity, contact angle, and electrical conductivity for oxidation and reduction of both oils, before their use in the electro-discharge machining process. Based on experimental tests, the Gr. mixed EDM oil has a 47.27% lower breakdown voltage, 6.22% higher thermal conductivity, 30% higher viscosity, and a 24.94% higher contact angle, with electrical conductivity 3.8 times higher (in oxidation and reduction) compared to EDM oil. This work enumerates both dielectric properties before their utilization in the EDM process. In the second stage, both dielectrics are used in the electro-discharge machining process. Parametric range values are selected based on performance in pilot experiments. Main experiments are conducted using Box-Behnken Design (BBD) with 27 run orders, and their performance is recorded in terms of output responses. Material Removal Rate (MRR) is improved by 36.44%, Tool Wear Rate (TWR) is reduced by 30%, Surface Roughness (SR) is enhanced by 2.58% and Hardness is reduced by 6.25%. It is observed that the combined desirability of G.M EDM oil 0.891 is better than EDM oil of 0.796.
77.	Interplay of exchange and anisotropy energies in landscape of current-driven skyrmion in defect-engineered racetracks **P Kamal, D Roy** - physica status solidi (RRL) - Rapid Research Letters, 2026 **Abstract:** Racetrack geometries provide a versatile framework for the creation of stable, nanometer-scale magnetic skyrmions that possess potential for future spintronic applications. For memory device applications, comprehension of the energy dynamics regulating the stability of an isolated skyrmion in environments abundant with defects is crucial. This study examines the temporal and spatial evolution of exchange, anisotropy, and total energy contributions during the current-generated motion of an isolated skyrmion in a racetrack with defects both smaller and greater than the size of skyrmion. Using micromagnetic simulations, we show that the behavior of the exchange energy is independent of defect size, exhibiting a temporal increase with defect number, while its spatial variation is governed by local skyrmion–defect interactions. In contrast, the anisotropy energy is defect-size dependent: For small defects, it is controlled by local skyrmion–defect interactions, whereas for large defects, it scales with the number of defects. The presence of defects leads to a higher total energy compared to a defect-free racetrack. Small defects act as low-energy pinning sites, while large defects induce global deformation and must be carefully optimized for efficient skyrmion transport.
78.	Isospin influence on the decay modes of compound nuclei $^{58-61}Cu^{*}$ N Kaur, **M Kaur**… B Singh - Nuclear Physics A, 2026 **Abstract:** Isospin influence on the decay of hot and rotating compound nuclei $^{58-61}Cu^{*}$ formed in the reactions $^{23-26}Mg+^{35}Cl$ at $E_{c.m.} \sim 32$MeV is investigated using the quantum mechanical fragmentation theory based dynamical cluster-decay model (DCM). Using this formalism, the calculated potential energy surfaces, carrying the structural effects, give the preformation probability, P_0 for a given decay mode which quantifies the prospects of a fragment being preformed before tunneling through the potential barrier, with certain penetration probability, P. In terms of these two quantities P_0 and P, the comparative contributions of the light particles (LPs, $A \leq 4$), light intermediate mass fragments (LIMFs, $5 \leq A \leq 12$), heavy intermediate mass fragments (HIMFs, $13 \leq A \leq 20$) and symmetric mass fragments (SMFs, $21 \leq A \leq A_{CN}/2$) in the total fusion cross-sections, σ_{fus}, have been calculated. The influence of degree of isospin has been seen on the fragment mass distribution, evaporation/ emissions of the LPs and the binary decay processes

	(LIMFs, HIMFs and SMFs) of the isotopic compound systems. The decay cross-sections for the dominant decay channels of LPs (σ_{LPs}) and LIMFs (σ_{LIMFs}) are added to give the DCM calculated σ_{fus}^{DCM} values which are in good comparison with the available experimental data as well as Hauser-Feshbach statistical model calculations.
79.	Lactobacillus plantarum as a novel modulator of immune and behavioral recovery in substance use disorders: a hypothesis **JA Malik** - Current drug research reviews, 2026 **Abstract:** Substance Use Disorders (SUDs) are increasingly recognized as conditions driven by neuroimmune dysfunction, leading to neuroinflammation and immune dysregulation. Growing evidence highlights the microbiota-gut-brain axis as a critical regulator of central nervous system activity, particularly through the modulation of glial cells such as microglia and astrocytes. The gut microbiome provides key immunomodulatory signals, and its therapeutic exploitation through probiotics offers a promising avenue. In this study, we hypothesize that supplementation with Lactobacillus plantarum can attenuate neuroinflammation and improve immune tolerance in SUDs by restoring microbial balance and modulating neuroimmune activity via the gut-brain axis. Using an established animal model of SUD, we propose to investigate the impact of L. plantarum on gut microbial composition, systemic and central inflammatory markers, glial cell activation, and behavioral outcomes. We further suggest that probiotics containing Lactobacillus species, including L. plantarum, could serve as a transformative approach not only for SUD-associated neuroinflammation but also for other neurological disorders. Such interventions may represent a breakthrough in non-drug discovery strategies by reducing reliance on conventional pharmacological treatments. Importantly, probiotic-based therapies could enhance overall survival and quality of life in individuals with SUDs, as Lactobacillus species have been shown to suppress inflammatory pathways from early developmental stages. Lactobacillus species could regulate the gut-brain axis and impact neurodegenerative diseases. If validated, this work could position L. plantarum and related probiotic strains as novel microbiome-based adjuncts for managing SUDs and open broader therapeutic possibilities for neuropsychiatric and neurodegenerative conditions.
80.	Laminar free convection from isothermal spherical segments in viscous newtonian and bingham plastic fluids **P Suri, SA Patel, T Mondal,** RP Chhabra - Industrial & Engineering Chemistry Research, 2026 **Abstract:** Extensive results on free convection heat transfer from a range of isothermal spherical segments in Bingham plastic fluids are presented here based on the numerical solution of the governing momentum and energy equations. The detailed kinematics as well as the gross macroscopic heat transfer behavior is strongly influenced by the shape of the segment (value of α, angle subtended by the part removed from sphere) and kinematic parameters (Grashof number, *Gr*; Prandtl number, *Pr*; and Bingham number, Bn). The present results are analyzed in terms of streamlines, isotherm contours, fluid-like (yielded) and solid-like (unyielded) subdomains, local and average Nusselt number elucidating the role of geometry (α = 30°, 60°, 90°, 120°, and 150°), Prandtl number (0.72–100), Grashof number (1–10^4), and Bingham number (0–10^5), including the limiting case of Newtonian fluid behavior (Bn = 0). Unlike in the case of Newtonian fluids, for Bingham plastic fluids, unyielded and yielded subdomains coexist in the flow domain depending upon the magnitude of the local stress tensor vis-a-vis the Bingham yield stress of the fluid. Broadly, increasing Grashof and Prandtl numbers augment heat transfer due to the increasing extent of yielding of the fluid in the flow domain, especially close to the solid–fluid interface. However, this potential advantage is countered by the increasing Bingham number, which suppresses fluid-yielding. Similarly, the increasing degree of bluntness of the spherical segments promotes fluid yielding and hence heat transfer. However, for fixed values of α, *Gr*, and *Pr*, there also exists a limiting Bingham number beyond which the entire body of fluid remains unyielded

	and therefore, heat transfer occurs solely by conduction under these conditions. This paper is concluded by presenting a couple of simple predictive equations for a priori estimation of the average Nusselt number in a new application, and the present results are compared with the experimental data as much as possible. 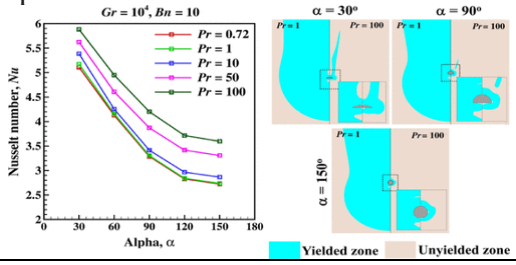
81.	Lower-Bound Finite-Element limit analysis of axisymmetric active earth pressure incorporating shear strength nonlinearity of soils **R Ganesh** - International Journal of Geomechanics, 2026 **Abstract:** For evaluating active earth pressures under plane strain conditions, extensive studies are available. However, research on axisymmetric active earth pressures remains limited and mostly employs the linear Mohr–Coulomb yield criterion, which does not account for the apparent shear strength nonlinearity exhibited by actual soils. In the present research, by considering a nonlinear power-type yield function, the axisymmetric active earth pressures against circular retaining walls are computed using a two-dimensional axisymmetric lower-bound limit analysis formulation combined with finite elements and second-order cone programming. The analysis was performed using an iterative numerical procedure. The effectiveness of using the nonlinear yield criterion was demonstrated through a comparative analysis, with the results obtained using the linear yield criterion for four different cohesive soils. A parametric study was further carried out to demonstrate the influence of various parameters, such as ground surface inclination angle, wall height, radius at the wall crest, soil–wall interface strength reduction factor, wall inclination angle, and surcharge pressure along the ground surface, along with tensile strength, nonlinearity coefficient, initial cohesion, and unit weight of soil backfill, on the axisymmetric active earth pressure against circular retaining walls. The study also examined the typical failure mechanisms associated with circular retaining walls for selected cases. The results obtained from the present study demonstrate considerable influence of shear strength nonlinearity of soils and compare favorably with existing numerical solutions reported in the literature.
82.	Mechanistic insights into the corrosion of heat-treated wollastonite-zirconia coatings reinforced with carbon nanotubes A Kumar…**R Kant, H Singh,** M Vostrak, S Houdkova - Ceramics International, 2026 **Abstract:** This research work investigates the corrosion behavior of as-deposited and heat-treated wollastonite-zirconia (WaZr) composite coatings, including those enhanced with carbon nanotubes (WaZr-CNT), and compares these against established hydroxyapatite (HA) coatings. The investigated coatings were deposited on titanium substrates using plasma spraying method. Microstructural investigations reveal that the addition of CNTs results in a denser and more uniformly bonded WaZr-CNT coating. Moreover, the coatings became denser after heat treatment due to effective melting of splats. Electrochemical impedance spectroscopy (EIS) indicates that HA coatings maintain superior performance under EIS tests. Nevertheless, potentiodynamic polarization tests show that the WaZr coatings achieve a substantial decrease, approximately 80%, in corrosion current density and about 70% in corrosion potential relative to HA coatings. The reinforcement with CNTs, however, leads to an increase in corrosion current density and a shift towards more negative corrosion potentials. Heat treatment of these coatings resulted in inferior performance despite better microstructure. To elucidate the underlying corrosion mechanisms,

	SEM, XPS, and XRD analyses were employed. A novel aspect of this study is the first-time application of electrochemical corrosion testing on CNT-reinforced WaZr coatings with and without heat treatment, revealing effect of CNT addition and heat treatment on corrosion resistance.
83.	Mitigating EMI susceptibility in three OpAmp INA with a high CMRR EMI immune OTA **Shivdeep, S Sharma, M Sakare, DM Das** - IEEE Transactions on Electromagnetic Compatibility, 2026 **Abstract:** Operational transconductance amplifiers (OTAs) are susceptible to conducted electromagnetic interference (EMI) reaching their input terminals. A DC OOV is generated, and it shifts the biasing of the circuit, which may cause an erroneous output or saturation in the worst case. The three-OpAmp instrumentation amplifier (INA) is widely used in analog front-end circuits for sensor interfacing, where the common-mode rejection ratio (CMRR) is an important performance specification. This article investigates the EMI-susceptibility of the three-OpAmp INA and presents an EMI-immune two-stage OTA with Miller compensation design to minimize the EMI-induced offset voltage in the three-OpAmp INA. The CMRR and in-band offset of the INA are taken into consideration along with EMI immunity. High CMRR of 81 dB and low in-band offset voltage of 298 V of the EMI-immune INA is measured on the IC fabricated using UMC 180 nm CMOS technology.
84.	Modeling and investigating the interactive role of fluid velocity and pore pressure within the lacunar-canalicular system in load-induced osteogenesis **H Shekhar, J Prasad** - Bone, 2026 **Abstract:** Current models propose that osteogenesis occurs in regions of high mechanical stimuli such as strain, fluid velocity, or pore pressure. However, in vivo experiments on mouse tibiae subjected to cantilever loading revealed new bone formation exclusively on the anterolateral side, although the opposite posteromedial surface experienced comparable magnitudes of these stimuli. This indicates that individual stimulus magnitude is insufficient and indicate an interactive mechanism.To investigate this, a poroelastic finite element model was developed to quantify the combined effects of load-induced fluid velocity and pore pressure. Tensile loading generated negative pore pressure that stretched osteocyte processes, whereas compressive loading produced positive pore pressure that compressed them. Because fluid flow exerts drag forces that also stretch osteocytes, the combined effect of flow and negative pressure on the tensile side was hypothesized to enhance mechanotransduction and trigger osteogenesis.Four candidate stimuli were evaluated: dissipation energy density arising from (i) pore pressure, (ii) fluid velocity, (iii) their non-interactive sum, and (iv) their interaction. Comparison with in vivo data showed that only the interactive dissipation energy density accurately predicted both the spatial pattern and the average rate of new bone formation per unit bone surface under high, low, and rest-inserted cantilever loading. The model also predicted osteogenesis under axial loading, demonstrating robustness.These findings advance mechanistic understanding by establishing that the interaction between fluid velocity and pore pressure, rather than their independent effects, governs load-induced osteogenesis, and provide a predictive basis for optimizing mechanical and clinical interventions to promote bone formation and mitigate bone loss.

	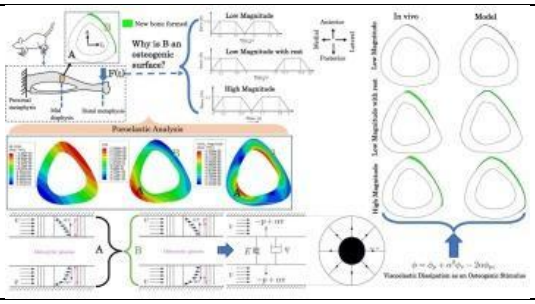
85.	On arithmetic nature of *q*-analogue of the generalized stieltjes constants **T Chatterjee,** S Garg - Integral Transforms and Special Functions, 2026 **Abstract:** In this article, our aim is to extend the research conducted by Kurokawa and Wakayama in 2003, particularly focusing on the q-analogue of the Hurwitz zeta function. Our specific emphasis lies in exploring the coefficients in the Laurent series expansion of a q-analogue of the Hurwitz zeta function around s=1. We establish the closed-form expressions for the first two coefficients in the Laurent series of the q-Hurwitz zeta function. Additionally, utilizing the reflection formula for the digamma function and the identity of Bernoulli polynomials, we explore transcendence results related to (Formula presented.) for q>1 and 0<x<1, where (Formula presented.) is the constant term which appears in the Laurent series expansion of q-Hurwitz zeta function around s=1. Furthermore, we put forth a conjecture about the linear independence of special values of (Formula presented.) along with 1 at rational arguments with co-prime conditions, over the field of rational numbers. Finally, we show that at least one more than half of the numbers are linearly independent over the field of rationals.
86.	Onomatopoeia in Maithili: A correspondence analysis in optimality theory **P Kumari, S Kar** - Journal of Universal Language, 2026 **Abstract:** The linguistic phenomenon of onomatopoeia, which mimics natural sounds, enriches language's expressiveness and exhibits consistent patterns across human languages. This study analyzes onomatopoeia in Maithili, a language that is spoken in the Mithila region of India and the Terai region of Nepal. The data collected in the field from native speakers of Maithili served as the primary data source, and a raw corpus of Maithili served as the secondary data source, providing a comprehensive list of onomatopoeic expressions in this language. The methodology adopted in this study uses qualitative analysis and descriptive frequency count. It also includes interviews, participant observation, and analysis of literary sources. The study examines the categorization of onomatopoeia and its analysis in Maithili within the framework of Correspondence Theory, a sub-theory of Optimality Theory. The findings reveal that onomatopoeic expressions in Maithili often intersect with reduplication, either entirely or partially, and in some cases, the interaction of reduplication is not observed. Completely reduplicated onomatopoeias are the most frequent, unlike the other two.
87.	Optimized wedged micropillar wick for simultaneous enhancement in evaporative heat flux and heat transfer coefficient **S Anand, CS Sharma** - International Journal of Heat and Mass Transfer, 2026 **Abstract:** Capillary-fed thin-film evaporation from well-defined micropillar wicks is a promising approach for microprocessor thermal management. In this work, we demonstrate that a micropillar wick, wherein each micropillar is equipped with wedges around its circumference, can be designed to achieve exceptionally high evaporative cooling performance compared to conventional cylindrical micropillar arrays. We systematically evaluate the effect of micropillar geometry on the liquid-vapour meniscus morphology which governs the evaporative cooling performance in terms of capillary pumping pressure and wick permeability. We optimize the wick design in order to maximize the evaporative heat flux dissipation and heat transfer coefficient, while imposing

	explicit constraints on wall superheat to avoid boiling incipience in the wick and limit the electronic device temperature within the safe operating limit. For water as the working fluid at saturation condition of 100°C, we find that imposing these wall superheat constraints yields an optimized wedged-micropillar design that can achieve more than 300% simultaneous enhancement in maximum heat flux and average heat transfer coefficient, compared to conventional cylindrical micropillars, without reaching the dryout condition. Even at reduced saturation conditions of 24°C, corresponding enhancements of 38% can be attained. This optimized wick design consists of wedged micropillars with twelve wedges per micropillar and optimal ratios of micropillar interstitial pitch and height to micropillar nominal diameter of ~1.5 and ~2 respectively. We also elucidate guidelines for designing wedged micropillar wick for achieving optimum thermal performance while accounting for the constraints imposed by the fabrication process.
88.	Organophotoredox-catalyzed vinyl group transfer reaction: an introduction to 4-Vinyl-1, 4-dihydropyridines **AK Mandhotra, SS Aristha, A Chakraborty, S Patel, I Chatterjee** - Organic Letters, 2026 **Abstract:** The visible-light-driven, organophotoredox-catalyzed vinyl group transfer reaction is described. The strategic use of proaromatic, bench-stable, and readily prepared 4-vinyl-dihydropyridine (DHP) derivatives triggers the vinyl group transfer that can couple stereoselectively with fluorinated esters and amides to forge the C(sp^3)–C(sp^2) bond. The obtained products are transformed into diverse fluorinated scaffolds. Preliminary mechanistic investigations are outlined. 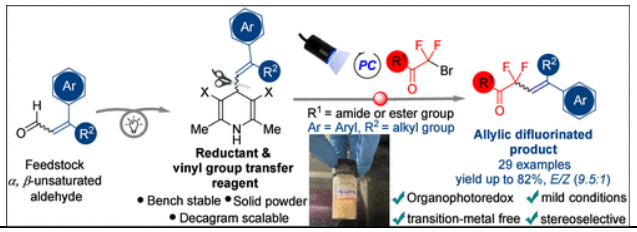
89.	Performance investigation of HfO X-based 1Transistor-1Memristor cell for in-memory logic gates implementation **MS Yadav, S Gupta, AK Gupta, B Rawat** - IEEE Journal on Emerging and Selected Topics in Circuits and Systems, 2026 **Abstract:** The transistor–memristor (1T-1M) integration has been recognized as an effective strategy to suppress crosstalk between neighboring cells for the development of a practical crossbar architecture, though its adoption for in-memory Boolean logic gate implementation is still missing. In this regard, we systematically investigate HfOX-based 1T-1M cell for in-memory logic gates implementation employing the Memristor-Aided loGIC (MAGIC) design style. This performance analysis is carried out using a fully calibrated and physics-based Stanford-PKU model, which captures full I–V switching dynamics, including temperature and stochastic effects. Our results show that the 1T-1M cell with the Gate and Source-controlled Off-State RESET (GSOSR) scheme substantially increases the high resistance state (HRS), which enables nearly 2.2× higher on-off resistance ratio compared to the 1M cell and achieves significant energy saving in execution operation for AND, NAND, XOR, and XNOR gates. Despite the 1T-1M cell exhibiting a slight increase in delay due to additional capacitances, the associated energy reduction and improved reliability outweigh this penalty. Variability analysis further reveals that the XOR gate with 1T-1M cell suppresses resistance fluctuation in both low resistance state (LRS) and HRS by up to 3× under worst-case corners, which ensures more robust operation over 1M cell. Overall, our findings demonstrate that the 1T-1M cell offers a viable path toward a scalable, energy-efficient, robust, and crossbar-compatible in-memory computing system, surpassing the widely employed 1M cell architecture.

90.	Performance of GFDM system over η− λ− μ fading channel for 6G communication **S Kalsotra…**P Kumar - International Journal of Electronics and Communications, 2026 **Abstract:** This article derives exact and asymptotic closed-form expressions for the average symbol error rate (ASER) of the generalized frequency division multiplexing (GFDM) system and space time coded (STC)-GFDM over the — fading channel. The analytical expressions are obtained using the moment-generating function (MGF) approach which provides a mathematically tractable and computationally efficient framework compared with conventional probability density function (PDF)-based methods that often involve complicated integrations. The derived results are verified through consistency with known Rayleigh and Nakagami- cases. Furthermore, the asymptotic analysis offers valuable insight into the system's diversity behavior at high SNR, making the proposed formulation a useful tool for GFDM performance assessment in next-generation wireless systems.
91.	Physics integrated adaptive residual learning framework for traffic state estimation **NK Pande, A Kumar, AK Gupta** - Engineering Analysis with Boundary Elements, 2026 **Abstract:** Due to rapid urbanisation, the development of Intelligent transport systems (ITS) has become extremely crucial. One of the key characteristics of ITS is traffic state estimation (TSE), i.e. the reconstruction of global variables like speed, density, flow, etc. In this work, a new TSE model utilising a residual learning framework with adaptive residual connections is integrated with the higher-order velocity gradient model of traffic flow. The robustness of the proposed model is verified on both the periodic and open boundary conditions. Various simulated traffic flow scenarios, like the development of shock and rarefaction waves and the stop-and-go traffic leading to the formation of the local clusters on the road, have been studied. The experimental results suggest that the proposed model efficiently learnt all the traffic flow scenarios, including the formation of phantom traffic jams, the evolution of shock and rarefaction waves that arise in traffic flow. Gradient flow analysis indicates improved gradient propagation and stable training over existing physics based machine learning methods. The empirical observations indicate the proficiency of the proposed traffic state estimation model over the existing physics-informed deep learning TSE models in the reconstruction of the traffic variables, especially when the traffic observations are sparse.
92.	POLR1B-derived circular RNA hsa-POLR1B_0014 orchestrates RNA polymerase I transcription and oncogenic hallmarks in lung adenocarcinoma through miR-181b -5p-mediated regulatory networks **D Antil, M Sharma, K Arpita, S Naidu** - Cancer Research, 2026 **Abstract:** RNA Polymerase I (Pol I) transcription is hyperactive in lung adenocarcinoma (LUAD), underpinning various hallmarks of cancer, including therapeutic resistance. However, the molecular mechanisms, particularly the role(s) of non-coding RNAs, that couple the Pol I transcriptional machinery to oncogenic pathways remain poorly defined. Here, we identify hsa-POLR1B_0014, a circRNA derived from POLR1B gene encoding the core subunit of Pol I, is up-regulated in LUAD in concert with its parent gene. RNA-sequencing analysis of a stable hsa-POLR1B_0014 knockdown LUAD cell line (A549) revealed upregulation of several miRNAs associated with oncogenic pathways. Among these, miR-181b-5p emerged as a key effector predicted to regulate LUAD-relevant malignant networks. Consistently, integrative analyses of public transcriptomic datasets, and LUAD tissues confirmed miR-181b-5p downregulation in LUAD. Furthermore, back-splice junction pull-down and AGO2-RNA immunoprecipitation assays validated a direct interaction between hsa-POLR1B_0014 and miR-181b-5p, with circRNA knockdown enhancing miRNA enrichment, thereby confirming its miRNA-decoy function. Functionally, loss of hsa-POLR1B_0014 elevated miR-181b-5p levels, leading to suppression of

	TAF1A, an essential Pol I transcription factor, thereby diminishing rRNA synthesis. This reveals a positive feedback circuit in which a Pol I-derived circRNA sustains Pol I output through sequestration of an inhibitory miRNA. Notably, miR-181b-5p also directly targets mTOR, a master regulator of Pol I transcription and malignant proliferation, inducing G1/S cell cycle arrest, apoptosis, and downregulation of Bcl2. Furthermore, miR-181b-5p suppression of ZEB1 attenuates migration, invasion, and enhances chemosensitivity to doxorubicin and cisplatin. In vivo, xenografts derived from hsa-POLR1B_0014-depleted LUAD cells exhibited markedly reduced tumor burden, rRNA synthesis, and Ki-67 expression, and increased apoptosis. Our findings uncover a previously unrecognized Pol I-derived circRNA-miRNA regulatory axis that coordinates ribosome biogenesis, cell growth, and therapeutic resistance in LUAD. By linking Pol I machinery to multiple oncogenic pathways, hsa-POLR1B_0014 emerges as both a driver and a vulnerability within the cancer Pol I network. These results highlight circRNA-mediated regulation of Pol I transcription as a central node controlling cancer hallmarks and a promising therapeutic target in LUAD.
93.	Q-RSMA based UAV-assisted vehicular cooperation: A finite blocklength perspective **S Bhattacharyya, S Kumar,** P Kumar, **S Darshi, B Kumbhani** - IEEE Transactions on Vehicular Technology, 2026 **Abstract:** The rising demand for ultra-reliable and low-latency communication (URLLC) in vehicular networks calls for solutions beyond traditional cooperative schemes. Next-generation multiple access techniques, such as rate-splitting multiple access (RSMA), offer a promising path to meet these stringent requirements. However, conventional RSMA-based cooperation systems suffer from error propagation due to successive interference cancellation (SIC). To mitigate this, we propose a novel quadrature rate-splitting aided multi-user cooperative (QRSMUC) system, where an unmanned aerial vehicle (UAV) serves as a relay and employs quadrature rate-splitting multiple access (Q-RSMA) as the relaying scheme. Unlike conventional RSMA-based cooperation, Q-RSMA eliminates SIC by orthogonally transmitting common and private streams, thereby enhancing spectral efficiency and reducing error propagation. To better align with the latency and reliability demands of next-generation vehicles (NGVs), we analyze the proposed system under a finite blocklength (FBL) regime, considering both perfect channel state information (pCSI) and imperfect channel state information (ipCSI) to capture realistic short-packet communication scenarios. An end-to-end analytical framework of the average block error rate (ABLER) is developed. The proposed QRSMUC system is compared with other systems across various metrics like ABLER, latency and reliability. The results obtained in MATLAB reveal that QRSMUC outperforms the existing benchmarks and achieves the URLLC conditions of 1 msec latency and 99.99% reliability at lower power levels. These results demonstrate the proposed system's strong potential in meeting the stringent quality-of-service (QoS) requirements of NGVs and other URLLC application scenarios.
94.	Reductive photocatalysis unlocks the hydrodeoxygenation of polycarbonate plastic into fuel-range hydrocarbons **R Ghalta, A Chauhan,** D Raj Deka…**R Srivastava** - Angewandte Chemie, 2026 **Abstract:** Polycarbonate (PC) is among the most challenging plastics to recycle because its robust aromatic C─O linkages resist conventional depolymerization strategies. Here, we report the first visible-light-driven photocatalytic system for the reductive depolymerization and hydrodeoxygenation of PC under ambient conditions, selectively producing propane-2,2-diyldicyclohexane (DCHP), a saturated hydrocarbon relevant to jet fuel applications. A multifunctional Ru@P-CHS(g-C_3N_4) catalyst integrates light harvesting, electron mediation, acidity, and hydrogen activation, enabling near-quantitative conversion of bisphenol A with ~94% molar selectivity toward DCHP. The catalyst also efficiently depolymerizes a range of real-world

	PC waste. Mechanistic investigations, including in situ UPS, kinetic isotope effect measurements, H_2─D_2 scrambling experiments, and DRIFT-IR spectroscopy, reveal light-driven electron accumulation at Ru sites and the formation of Ru─H intermediates, confirming illumination-induced H_2 activation at Ru that drives C─O bond cleavage. This work establishes a sustainable strategy for converting end-of-life plastics into fuel-range hydrocarbons and introduces reductive photocatalysis as a new paradigm for plastic upcycling. 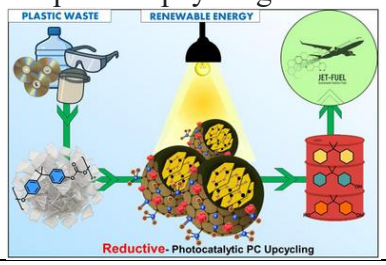
95.	Remote sensing-based multi-criteria astronomical site suitability mapping in the north west Himalayas S Ray…**S Sharma,** MO Sarif - Journal of the Indian Society of Remote Sensing, 2026 **Abstract:** This research work presents a comprehensive assessment of the Astronomical Observation Site (AOS) suitability map using fuzzy logic in a GIS-based environment for the North West Himalayan Mountain (NWHM) region. Multi-temporal climatic data from 2002 to 2022, and remote sensing (RS) data have been used to derive a total of nine selected factors, which are Elevation (EL), Slope (SL), Normalised Difference Vegetation Index (NDVI), Temperature (TEMP), Relative Humidity (RH), Precipitation (PR), Cloud Amount (CL), Aerosol Optical Depth (AOD), and Night-time Light (NTL). All the parameters were normalised using fuzzy membership functions based on their influence on Astronomical Observation (AO). Fuzzy gamma operation was adopted to utilise data uncertainty and interdependency effectively. The gamma integration was performed for nine different gamma values (range: 0–1), and gamma value 0.9 was selected for the development of the final suitability map. The resulting map was reclassified into five categories from very less, less, moderate, suitable, and very suitable, based on natural breaks, and a sixth class represents the waterbodies and permafrost. To validate the performance, a machine learning evaluation technique with the help of the Receiver Operating Characteristic (ROC) curve analysis has been taken into consideration to demonstrate high predictive accuracy for selected different gamma values. The methodology validates the existing sites and locates several unexplored, highly-potential areas for the development of AO. It highlights the effectiveness of fuzzy logic for AOS selection for planning in a complex geographic, climatic, and ecologically sensitive mountain region such as NWHM. The methodology shows flexibility and adaptability for future changes, supporting spatial decision-making.
96.	Revisiting inflation-growth nexus through the lens of price-stickiness: Evidence from India and Indonesia **B Garg,** PK Narayan, **SA Shah,** F Indawan - Applied Economics, 2026 **Abstract:** This paper examines the inflation – growth nexus in India and Indonesia through a dynamic stochastic general equilibrium (DSGE) framework. Employing quarterly data from 2009Q1 to 2024Q4 , the model incorporates high and low price-stickiness scenarios to capture asymmetries in inflation – growth dynamics. The results indicate that not only the state of the economy but also the nature of shocks plays a crucial role in shaping inflation outcomes. Specifically, higher price-stickiness enhances the effectiveness of monetary policy in stabilizing inflation, albeit at the cost of higher output losses. Unlike demand shocks, supply shocks exert stronger inflationary pressures under higher price stickiness. These findings underscore the importance of price rigidities and shock characteristics in macroeconomic dynamics, offering

	actionable insights for emerging markets policymakers seeking to balance inflation control and growth.
97.	Robotic systems in internet of things: Addressing security challenges through threat modeling and penetration testing **MR War,** A Sayeed, SA Wani, A Lone, MS Mir, Y Gulzar - Scientific Reports, 2026 **Abstract:** The increasing prevalence of robotic systems across diverse domains has undoubtedly delivered numerous advantages. However, this proliferation has also exposed these systems to potential security threats, with the ability to cause significant human and financial losses. In this study we propose a proactive approach to risk management using threat modeling techniques. This approach provides a systematic framework for risk assessment, facilitating the identification and prioritization of the most severe threats for possible mitigation. Specifically, we provide Attack-Defense Tree (ADT) based methodology, an extension of the conventional tree formalism which incorporates mitigation nodes representing applicable counter measures at different hierarchical levels. This enhancement enables a comprehensive and structured analysis of security risks. The proposed ADT-based approach is tailored to reinforce the security of the camera component within robotic systems operating on the Internet of Robotic Things (IoRT) environment. Additionally, penetration testing is conducted to empirically evaluate the vulnerability of robotic devices to flooding-based denial-of-service (DoS) attacks. Experimental validation using the AlphaBot platform demonstrates the feasibility of executing a successful DoS attack on its camera module. These findings underscore the urgent need for anticipatory security strategies in IoRT systems and highlight the critical importance of robust, preemptive threat modeling to ensure cyber-resilience in modern robotic infrastructures.
98.	Selectfluor-promoted transition metal-free tunable reactivities of thio-oxindoles: Synthesis of disulfanes and 2-oxindoles **M Lamba, M Kumar, R Das, A Goswami** - European Journal of Organic Chemistry, 2026 **Abstract:** An efficient and operationally simple protocol for the synthesis of disulfanes and 2-oxindoles mediated by selectfluor under metal-free conditions is described here. The methodology proceeds under mild reaction conditions and exhibits broad substrate scope, delivering the corresponding disulfane and 2-oxindole derivatives in good to excellent yields. 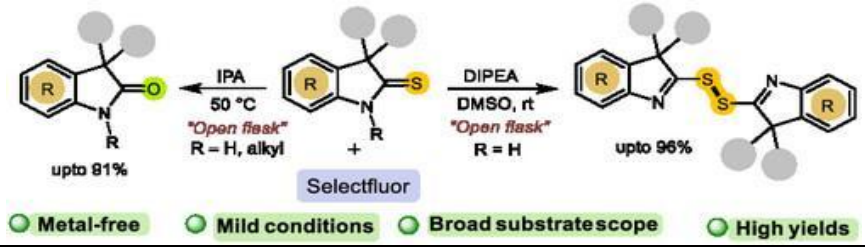
99.	Selective depletion of virus-specific CD8 T cells from the liver after PD-1 therapy with Fc-intact antibody during chronic infection M Hashimoto…**MA Khan,** Z Peng - National Academy of Sciences, 2026 **Abstract:** Anti-programmed cell death 1 (PD-1) antibody therapy is now widely used in various cancers. However, the role of the antibody Fc region in PD-1 directed immunotherapy is not well understood. Preclinical studies commonly use species-mismatched rat anti-mouse antibodies, which may not accurately reflect antibody-Fc gamma receptor (FcγR) interactions. Here, we used mouse anti-mouse PD-1 antibodies to investigate how the Fc region influences therapeutic efficacy for enhancing CD8 T cell responses using mouse models of chronic lymphocytic choriomeningitis virus infection and CT26 tumors. Treatment with these mouse anti-mouse PD-1 antibodies caused preferential depletion of PD-1+ virus-specific CD8 T cells in the liver, resulting in increased viral

	titers. These effects of mouse anti-PD-1 antibodies were Fc dependent since mutating the Fc region to block FcγR interaction prevented PD-1+ CD8 T cell depletion and resulted in effective immunotherapy. Using mice lacking activating FcγR III or inhibitory FcγR IIb, we found that depletion of PD-1+ CD8 T cells was mediated via activating FcγR III. Furthermore, we determined that phagocytic cells, not natural killer cells, were the in vivo effectors that mediated depletion of PD-1+ CD8 T cells. Similar depletion of tumor-specific CD8 T cells and reduced tumor control were observed in the CT26 model with Fc-intact mouse anti-mouse PD-1 treatment. These findings highlight potential negative effects of Fc-functional anti-PD-1 antibodies in therapies for liver cancer, liver metastases, and chronic hepatotropic viral infections. Conversely, FcγR-mediated depletion could benefit "agonistic" anti-PD-1 antibodies for treatment of autoimmunity. Our research emphasizes the importance of Fc region in tailoring PD-1 therapies for diverse clinical applications.
100.	Selective hydrogenation of furfural to 2-methyltetrahydrofuran over bimetallic Ru–Ni nanoparticles supported on nanocrystalline CeO2 **BP Singh,** R Bal, **R Srivastava** - ACS Applied Nano Materials, 2026 **Abstract:** Nanocrystalline ceria (CeO_2) with engineered surface defects provides a versatile platform for constructing catalytically active metal-oxide interfaces. Herein, we report defect-rich nanocrystalline CeO_2-supported bimetallic Ru–Ni nanoparticles, in which electronically coupled interfacial sites govern selective biomass upgrading. Structural and spectroscopic analyses (XRD, TEM, XPS, EPR, Raman, H_2-TPR/TPD, and NH_3-TPD) reveal strong metal–support interactions, abundant oxygen vacancies, and nanoscale Ru–Ni proximity, which promote interfacial electronic coupling without alloy formation. The optimized 3Ru-5Ni/CeO_2 catalyst achieves complete conversion of furfural (FAL) with 92% selectivity toward 2-methyltetrahydrofuran (2-MTHF) at 200 °C and 0.5 MPa H_2 in 2 h. Reaction optimization, substrate transformation studies, kinetic studies, and pyridine poisoning experiments establish a sequential pathway involving FAL hydrogenation to furfuryl alcohol (FOL), its hydrodeoxygenation to 2-methylfuran (2-MF), and final ring hydrogenation to 2-MTHF. The enhanced performance originates from cooperative nanoscale interactions in which Ru facilitates H_2 dissociation, Ni promotes C–O bond activation, and vacancy-rich CeO_2 enables hydrogen spillover and intermediate stabilization. These findings demonstrate how defect engineering and bimetallic interface design in nanostructured oxide supports can precisely steer reaction pathways for sustainable upgrading of biomass-derived furans. 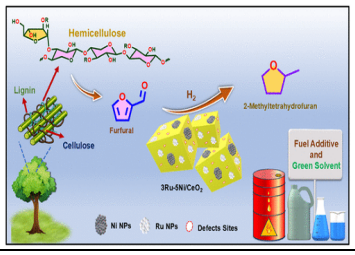
101.	Single-probe Pd-Modified ZnO–polymer fluorescent sensor array for discrimination of thymidine analogues in aqueous media K Gaur**, Ranbir,** N Kaur, **N Singh** - Analytica Chimica Acta, 2026 **Abstract:** Thymidine analogues are widely used as antiviral and anticancer agents; however, improper dosage and prolonged exposure can lead to severe hematological and genetic complications, necessitating reliable methods for their detection and discrimination. We report an array-based fluorescence sensing platform for the discrimination of structurally related thymidine analogues in aqueous media using a Pd-modified ZnO–polymer nanocomposite as a single cross-reactive probe. The nanocomposite was synthesized by functionalizing ZnO nanoparticles with a

	KG3 polymer matrix followed by palladium ion modification, and its structure and morphology were confirmed using standard spectroscopic and microscopic techniques. Distinct fluorescence response patterns were generated upon interaction with different thymidine analogues, enabling their effective differentiation through multivariate statistical analysis. Principal component analysis (PCA), linear discriminant analysis (LDA), hierarchical clustering analysis (HCA), and support vector machine (SVM) classification demonstrated reliable discrimination with high accuracy across the analyte set. The sensor array exhibited sensitive fluorescence responseswith limits of detection in the range of 6–100 μM. This approach demonstratesthe potential of single-probe fluorescence sensor arrays combined with pattern-recognition algorithms for the discrimination of closely related nucleoside analogues in complex chemical environments. 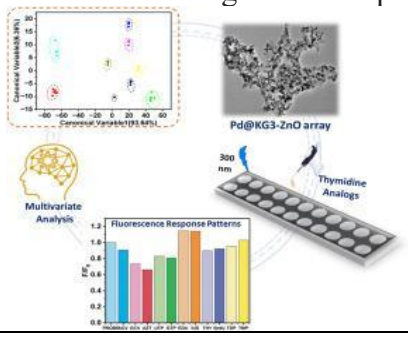
102.	SPIM: Split-packet interference management for uplink RSMA in next-generation wireless networks **S Bhattacharyya, S Darshi,** K Singh, B Clerckx - IEEE Transactions on Wireless Communications, 2026 **Abstract:** Driven by the growing demands for reliability and high data rates, uplink rate-splitting multiple access (RSMA) has emerged as a promising technique for next-generation wireless networks. However, in practical scenarios, particularly under imperfect SIC (ipSIC), the presence of residual interference (RI) significantly degrades performance, especially at high transmit power levels. This RI stems from two key sources: intra-user split packet interference (SPI) due to imperfect cancellation of a user's own split streams, and inter-user residual packet interference (IPI) from imperfect cancellation of other users' signals. As these impairments accumulate across multiple SIC stages, the inherent benefits of rate splitting may progressively diminish, potentially resulting in performance degradation compared to conventional schemes such as non-orthogonal multiple access (NOMA). To address this challenge, we propose a split-packet interference management (SPIM) framework that enhances uplink RSMA performance under ipSIC by structurally enforcing orthogonality between a user's own split streams. This design reduces the reliance on successive decoding and effectively limits the propagation of RI, especially from SPI, while preserving the benefits of rate-splitting. We consider a two-user system and perform a comprehensive outage probability analysis under both perfect SIC (pSIC) and ipSIC conditions, leveraging a copula-based statistical modelling framework to accurately model the dependency between streams. Additionally, we derive analytical expressions for the ergodic sum rate thus, providing insights into the long-term performance. While the core analysis focuses on a two-user setup, the SPIM RSMA architecture is extended to larger user groups with a scalable receiver design. Simulation results closely match analytical findings and demonstrate that while SPIM RSMA performs comparably to conventional RSMA under pSIC, it significantly outperforms both conventional RSMA and NOMA under ipSIC conditions in terms of outage probability, sum-rate, and sum-throughput. These results underscore the structural versatility of SPIM RSMA, which proactively mitigates SPI, thereby preserving the advantages of rate splitting in SIC-constrained environments.

103.	Strength characteristics of expansive soil stabilized with low-carbon wollastonite powder and polyester fibers KK Perigalla, **B Kamasani,** R Kumarakalva, **PK Revuru,** MR Kattamuri - Indian Geotechnical Journal, 2026 **Abstract:** Expansive soils exhibit significant volume changes due to moisture variations, necessitating soil stabilization. Conventional stabilizers, such as lime and cement, have environmental drawbacks due to their carbon emissions. In this study, wollastonite powder (WP), a natural silicate mineral, and polyester fiber (PF), a synthetic reinforcing material, were used to improve the strength properties of expansive soil. Experimental investigations were conducted on the collected soil samples with varying percentages of WP (0-12%) and PF (0.15-1%) were added at the optimum WP content of 6%. Laboratory tests were conducted according to Indian standards, such as Atterberg limits, compaction tests, and unconfined compressive strength (UCS) tests at curing days of 0, 7, and 14. The results indicated that adding WP significantly reduced the liquid limit and plasticity index while increasing the plastic limit of the soil. The maximum dry density decreased, and the optimum moisture content increased with the addition of WP. The UCS of soil with an optimum 6% WP increased four times compared to untreated soil with 14 days of curing. The incorporation of 0.5% PF with soil and 6% WP exhibited the highest improvement in UCS, 5-times more than that of untreated soil, after 14 days of curing. Cementation compounds were observed from scanning electron microscopy and X-ray diffraction. The combined use of WP and PF is an effective and eco-friendly method for improving the mechanical properties of expansive soil. A comparative CO_2 assessment indicates that wollastonite stabilization has a lower carbon footprint than lime and cement stabilization within the material-production system boundary.
104.	Substituent-induced modulation of proaromaticity in benzo-fused fluorenophenalene exhibiting low-lying LUMO **S Sahewal, S Sharma,** D Mallick, **S Das** - Chemical Communications, 2026 **Abstract:** Fluorenophenalene (**FP**) is an underexplored proaromatic polycyclic hydrocarbon. Herein, we report the synthesis of benzo-fused FPs bearing aryls (mesityl, $C_6H_2F_3$ and C_6F_5) of varying electronic character as apical substituents of the cyclopenta-unit with large HOMO/LUMO coefficients. Benzo-fusion expands the *p*-quinoidal conjugation length by forming a polyene-like subunit, while electron-deficient aryls improve the electronic communication. As a result, the HOMO–LUMO gap decreases as the core aromaticity increases. Replacing a mesityl pendant with C6H2F3 and C6F5 lowers the LUMO energy, steadily stabilizing it from −3.08 eV to −3.64 eV and −4.20 eV, respectively, highlighting our design efficacy.
105.	Sustainable ultrafine fly ash bricks with PCM microcapsules enhance indoor thermal regulation in hot climates AB Huluka, **S Muthulingam, S Manigandan** - International Journal of Thermofluids, 2026 **Abstract:** Fly ash bricks are promising sustainable materials for building envelopes; however, under high solar exposure, their sensible heat storage alone may be insufficient to limit indoor heat gain. As the demand for energy-efficient and sustainable building materials grows, there is a need for solutions that can improve the thermal performance of these materials. This preliminary study investigates the outdoor thermal performance of ultrafine fly ash bricks incorporating a surfactant-free silica-shell microencapsulated phase change material (MePCM), synthesized via Pickering emulsion, under hot climatic conditions. The thermal performance of these MePCM-integrated bricks was compared to conventional fly ash bricks without MePCM using several metrics, including temperature profiles, heat flux variations, attenuation index, thermal buffering capacity, decrement factor, and time lag. The MePCM-integrated brick maintained lower interior temperatures during the day, reducing the daily maximum interior temperature by up to 7.0 °C

	and, on average, by 3.6 °C. It also moderated heat-flow peaks, with peak heat flux decreasing by 23.1% and a mean daily peak heat flux attenuation index of 0.306. Time lag increased from 6.28-8.88 hr for the conventional brick to 8.58–11.95 hr for the MePCM-integrated brick, indicating stronger thermal inertia and delayed heat transmission. The results highlight the potential of MePCM-incorporated fly ash bricks as an effective passive cooling strategy for energy-efficient building design.
106.	Torsional-rotational floor acceleration amplification in RC buildings A Jain, **M Surana** - Structures, 2026 **Abstract:** The present study investigates floor acceleration response of reinforced-concrete moment-resisting frame buildings under the combined influence of building torsion and rotational ground motions. To achieve the aforementioned objective, the study adopts a hybrid approach, wherein the floor acceleration responses of 24 reinforced-concrete moment-resisting frame buildings are investigated numerically and compared with those obtained from instrumented building responses. The torsional-rotational amplification factor, defined as the ratio of the maximum to the average floor acceleration in the direction under consideration, is evaluated for the lightweight acceleration-sensitive rigid and flexible secondary systems and their relationships with the corresponding maximum to the average floor displacements are established. The derived torsional-rotational amplification factors for the instrumented buildings are found to be in reasonable agreement with those obtained for the investigated buildings. Simplified recommendations are proposed for the seismic design of lightweight acceleration-sensitive rigid and flexible secondary systems in torsionally irregular buildings.
107.	Transient deformation and charge evolution during alternating current-electrohydrodynamic oscillations of confined droplets **P Gupta,** P Dhar, **D Samanta** - Langmuir, 2026 **Abstract:** This study investigates the transient electrohydrodynamic behavior of a confined, neutrally buoyant droplet subjected to a cyclic electric field, focusing on the coupled evolution of interfacial charge, deformation, and flow. Both the droplet and the surrounding medium are modeled as Newtonian, immiscible leaky-dielectric fluids under creeping-flow and small-deformation conditions. Confinement is shown to significantly dampen droplet oscillations by enhancing viscous dissipation in thin fluid gaps, restricting internal and external circulation, and increasing hydrodynamic resistance that opposes electrically induced Maxwell stresses. The transient response is decomposed into mean and time-periodic components to examine two conductivity configurations, in which the droplet is either more or less conductive than the surrounding medium. The effects of confinement ratio, oscillation frequency, and electrical property contrasts are systematically analyzed to quantify their influence on deformation amplitude, flow-field strength, and interfacial stress balance. Increasing the confinement suppresses time-dependent deformation by limiting flow development and amplifying viscous resistance, leading to a marked reduction in oscillation amplitude. The role of the relaxation frequency in governing the electrical response is examined by distinguishing conduction- and displacement-dominated regimes. At low frequencies, rapid charge relaxation promotes strong interfacial charge accumulation and enhanced electrohydrodynamic forcing, resulting in pronounced deformation and circulation. At higher frequencies, displacement currents dominate, interfacial charge weakens, and both deformation and flow are attenuated, particularly under confinement. Phase lags between the applied electric field, interfacial charge, and electric fields inside and outside the droplet are quantified and shown to depend on confinement, fluid properties, and excitation frequency. The results provide physical insight into frequency-dependent electrohydrodynamic droplet dynamics in confined environments relevant to microfluidic and droplet-based technologies.

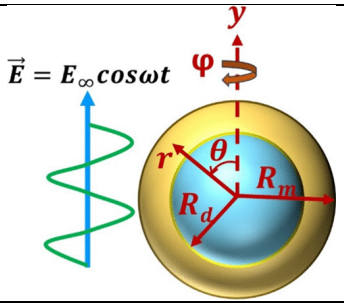

108. [Two-step strategy to design organo-fluorophore: Engaging palladium catalysis for carbo-oxygenative cyclization of chloroprene derivatives]
P Singh, SS Bisht, MV Mane, **JA Malik,** M Shankar, BS Naidu, **JN Agrewala, AC Shaikh** - Organic Letters, 2026

Abstract: Herein, we present a two-step protocol for the synthesis of an organo-fluorophore using palladium-catalyzed carbo-oxygenative cyclization of chloroprene derivatives. Protocol is well-tolerated with a broad substrate scope and is feasible at gram-scale synthesis. Mechanistic studies were conducted using H_2O^{18} labeling and density functional theory (DFT) analysis. Notably, organofluorophores show strong photoluminescence and fluorescence lifetimes along with notable redox potential. Furthermore, cell viability studies showed low toxicity and high selectivity for lysosomes, making them promising candidates for green lysotracker imaging agents.

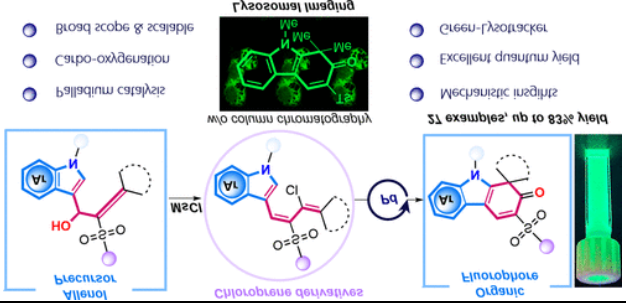

109. [Understanding the spectral acceleration amplification factors of reinforced concrete frames through explainable artificial intelligence]
I Latif, A Banerjee, **M Surana** - Computers & Structures, 2026

Abstract: Spectral acceleration amplification factors corresponding to fundamental (A_1) and second mode periods (A_2) are useful for designing connections of secondary systems with supporting structures. Their estimation is computationally intensive due to dependence on material, ground motion, and structural characteristics. We propose machine learning approach to understand and predict A_1 and A_2. The procedure involves obtaining 50 sets of material properties through Latin hypercube sampling to model 4-, 8-, and 12-storey reinforced-concrete buildings subjected to 30 pulse type earthquakes for obtaining A_1 and A_2 at varying strength ratios. The trained XGBoost models which performed the best among all investigated models were subjected to sensitivity analysis and explainable artificial intelligence method for understanding the effect of input features on the predictions. The structural characteristics are found as most important for predicting A_1 and A_2. The pulse period of ground motions is more important in predicting A_2 compared to A_1. Further, concrete properties are more critical for the predictions compared to steel. The prediction capabilities of trained models were compared with existing equations. The models provided reasonable performance for unseen buildings compared to existing equations. An interactive dashboard is also developed to obtain A_1 and A_2, enabling accurate and rapid predictions using the trained models.

110. [Unlocking ultra-low-power bluetooth low energy relays with periodic advertisements]
S Gautam, S Kumar, EE Tsiropoulou - IEEE Internet of Things Journal, 2026

	Abstract: This article demonstrates an unexplored relay operating mode in Bluetooth Low Energy (BLE)-based Wireless Sensor Networks, enabled by the link-layer synchronization inherent to BLE periodic advertisements. This synchronization allows relay nodes to avoid the power-hungry 100% duty primary-channel scanning that conventional passive BLE receivers rely on for reliable packet capture. To translate this insight into practice, we present the design and implementation of Dynamic Primary-Channel Scanning (DPCS), a practical strategy that disables primary-channel scanning after periodic synchronization and autonomously re-enables it upon synchronization loss, thereby allowing relay nodes to remain asleep for most of their lifetime while still forwarding data on scheduled secondary-channel receptions. We integrate DPCS into a multi-hop, chain-based data propagation framework for linear BLE-based WSNs, where sensor nodes themselves act as relays and forward concatenated data hop-by-hop toward a sink. Enabled by the innate properties of the periodic advertising mechanism, DPCS is directly deployable on commercial off-the-shelf (COTS) BLE 5.x devices as an application-level control logic using the provisions of the BLE stack. Experiments with nRF52832-based nodes in five-node chains demonstrate over 99% per-hop data reception reliability indoors across 50–60 m with modest retransmissions. In outdoor deployments, the per-hop reliability consistently remains above 99% without retransmissions across a 180–200 m span, with rapid automatic re-synchronization after interruptions. Power profiling shows consistently lower energy consumption than both continuous and duty-cycled primary-channel scanning baselines, with up to two to three orders of magnitude savings over continuous scanning at a sensing interval of 60 s. This chain-based analysis provides a baseline for extending the proposed periodic-advertising-based relay operation to more complex network topologies.
111.	Vehicle automation for safety and comfort: Familiarity, implementation, and willingness to pay among Indian consumers **Nikhil, TM Rahul** - Transport Policy, 2026 **Abstract:** Advanced Driver Assistance Systems (ADAS) play a pivotal role in enhancing road safety and driving convenience by reducing human intervention. However, their usage in India is currently limited to premium cars. This study investigates consumer familiarity with ADAS, their choice of ADAS implementation models (compulsory features, subscription-based services, and optional add-ons), and their preference for ADAS-equipped vehicles in the emerging market of Chandigarh, India. An ordinal choice model, an Integrated choice and latent variable (ICLV) model, and a hybrid choice model are respectively used to achieve these objectives. The latter model estimates the varied Willingness to pay (WTP) for ADAS features among different market segments. The current study extends existing literature on ADAS adoption by incorporating a reference-dependent framework that captures the non-linear cost perception among people. The data for the study were collected using a questionnaire survey that included stated choice experiments. Our findings reveal that the low-income group and females are less familiar with ADAS. Furthermore, higher levels of ambivalence among individuals were associated with a lower preference for the compulsory implementation of ADAS. Individuals were more likely to invest in driving control assistance features like adaptive cruise control than collision intervention systems. The WTP for ADAS features varied between 96953 Indian rupees (INR) (1117.02 USD) to 205971 INR (2373.05 USD) for market segments with varied purchasing power.
112.	Voltage-dependent capacitance as a measure of pore accessibility of supercapacitor electrodes K Chatterjee, B Sriram, **PK Agnihotri,** S Basu, N Gupta - IEEE Transactions on Instrumentation and Measurement, 2026 **Abstract:** Despite extensive research over the past two decades, achieving simultaneous high energy and power density in supercapacitors (SCs) remains a challenge. The key lies in designing nanoporous networks that offer a very high surface area while also maximizing electrolyte-ion

	accessibility of the pores. However, experimentally measuring pore accessibility in SC electrodes is challenging. This study employs a particle-in-cell (PIC)-based computational approach to simulate charge transport, governed by the Poisson–Nernst–Planck (PNP) equation, from the bulk electrolyte into porous electrodes. The influence of applied potential and pore morphology on charge dynamics of the SC is investigated. Results reveal that highly tortuous pores, along with low porosity, significantly reduce the charging rate. However, this adverse effect is mitigated by applying higher voltages, making initially inaccessible pores accessible, and thereby enhancing capacitance. Hence, the extent of voltage-dependence of capacitance is introduced as a measurable index for quantifying the pore accessibility in SC electrodes. Experimental validation confirms that this metric effectively distinguishes pore networks of various SC electrodes in terms of pore accessibility, using simple capacitance measurements. The proposed metric thus serves as a practical tool for designing high-performance SC electrodes for energy storage in electric vehicles (EVs) and renewable energy systems.
113.	Yukawa coupling, and inflationary correlation functions for a spectator scalar via stochastic spectral expansion S Bhattacharya, **S Kumar** - Journal of Cosmology and Astroparticle Physics, 2025 **Abstract:** We consider a stochastic spectator scalar field coupled to fermion via the Yukawa interaction, in the inflationary de Sitter background. We consider the fermion to be massless, and take the one loop effective potential found earlier by using the exact fermion propagator in de Sitter spacetime. We take the potential for the spectator scalar to be quintessence-like, $V(\phi)= \alpha\|\phi\|p$ ($\alpha >$ 0, $p > 4$), so that the total effective potential is generically bounded from below for all values of the parameters and couplings, and a late time equilibrium state is allowed. Using next the stochastic spectral expansion method, we numerically investigate the two point correlation function, as well as the density fluctuations corresponding to the spectator field, with respect to the three parameters of the total effective potential, α, p and the Yukawa coupling, g. In particular, we find that the power spectrum and the spectral index corresponds to blue tilt with increasing g. The three point correlation function and non-Gaussianity corresponding to the density fluctuation has also been investigated. The increasing Yukawa coupling is shown to flatten the peak of the shape function in the squeezed limit. Also in this limit, the increase in the same is shown to increase the local non-Gaussianity parameter.

Disclaimer: This publication digest may not contain all the papers published. The library has compiled the publication data as per the alerts received from Scopus and Google Scholar for the affiliation “Indian Institute of Technology Ropar” for the month of April, 2026. The author(s) are requested to share their missing paper(s) details, if any, for inclusion in the next publication digest.